國立中興大學化學工程學系
碩士學位論文

新式奈米碳管分散法

New Method of Dispersing Carbon Nanotubes

指 導 教 授：林 江 珍 博士

共 同 指 導：林 慶 炫 博士

研 究 生： 藍 伊 奮

中華民國 九十五 年 六 月

新式奈米碳管分散法

New Method of Dispersing Carbon Nanotubes

國立中興大學化學工程學系
碩士學位論文

題目：New Method of Dispersing Carbon Nanotubes

姓名：藍伊鳶　　學號：79365132

經口試通過特此證明

論文指導教授 林江珍 林慶炫

論文考試委員 蔣見超 范如忠

[illegible]

中華民國 95 年 6 月 7 日

Content

Abstract

We observe a geometric shapes difference which largely influences fine dispersion of carbon nanotubes (CNT) in several mediums such as water, ethanol, isopropyl alcohol, acetone, 2-butone (MEK), tetrahydrofuran (THF), toluene, dimethyl formamaide (DMF) and dimethyl aceticamide (DMAC). When the synthetic fluorine mica (Mica) of platelet shapes and ionic charged was pulverized with lengthy CNT, the physically mixed CNT-Mica hybrid exhibited a uniquely fine dispersion due to the redistribution of van der Waals bonding forces among these nano-materials. Two other clays including montmorillonite (MMT) and layered double hydroxide (LDH) were examined and the UV-vis results revealed the Mica is the most effective clay, because of its high aspect ratio and difference in geometric shape. The generated CNT-Mica hybrids have an amphiphilic property and irreversibly dispersing in either water or toluene, depending on the exposing order. According to the surfactant principle of O/W and W/O micelle formation, we proposed an influencing factor for the dispersion of nanomaterials and a new mechanism of geometric-shape controlling non-covalent bonding attraction. Ultraviolet-visible spectrophotometer provided an evidence of the micro-phase separation between CNT and Mica. Transmission electron microscopy was used to verify the fine dispersion in an irreversible manner. Sequentially, MWNT-Mica hybrid/PVA composites were prepared and demonstrated a high thermal degradation temperature, from 300^{o}C to 400^{o}C at 50 wt% loss by the standard TGA test.

1. Introduction

In 1959, Noble Prize winner in physics Richard Feynman stated “there is plenty of room at the bottom”, and predicted the arrival of the nano-technological times. However, with the progress of the scientific development, it is possible for human being to observe tiny particles from milli-scale to micro-scale. Furthermore, during 1980 to 1985, the IBM Lab invented the scanning tunnel microscope (STM) and atomic force microscope (AFM), which enable scientists to scrutinize the atomic particles and motivated an interest in exploiting nano-materials. Moreover, the nano-materials already originally exist in nature, for example, lotus effect and magnetic nano-particles inside the bees for guidance system.

Up to the present, there are varieties of nanomaterials that had been discovered and created. According to the geometric shape, those nano-materials can be classified into three categories: two dimension materials (e.g. layered silicates, (Figure 1(a))), one dimension materials (e.g. carbon nanotubes, (Figure 1(b))) and zero dimension materials (e.g. C_{60}, (Figure 1(c))). Among those nano-materials, carbon nanotubes (CNT) exhibit superior chemical and physical properties and are expected to have various applications such as conjugated polymer donor, field-emission display, biosensor, fuel cell membrane, etc.

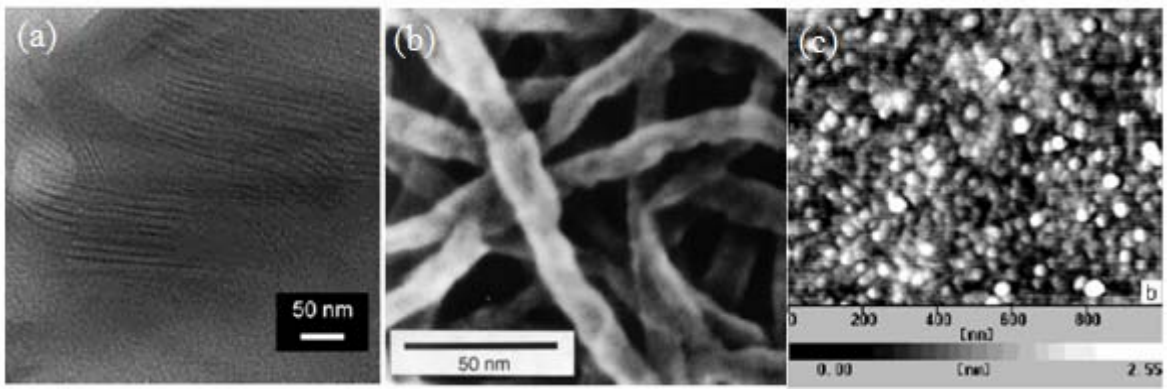

Figure 1. Mmorphology of nano-materials.(a) layered silicates[1], (b) carbon nanotubes[2], (c) C_{60}[3].

However, CNTs have large surface area and strong van der Waals attractions which resulted in large bundles and hindered the progress of many applications (Figure 2).[4,5] Several approaches of separating large bundles of CNT have been developed, including oxidation, atom transfer radical polymerization (ATRP), acylation-mediated amidation and carbodiimide-activated coupling, etc. Nevertheless, most of them are involved in chemical modification of CNT surface through covalent bonding at their side defect and destruction of the sp^2 structures in the graphite sheet associated with the formation of new covalent bonds on CNT surface, which are undesirable due to inevitable deterioration of the unique CNT properties. An alternative method, without the deterioration, is developed by using physisorption and ionic interactions. Surfactants and polymers are the most common materials for non-covalent bond absorption of CNT. However, it is necessary to adsorption plenty of surfactants or polymers in order to improve the dispersion of CNT. Recently, a grinding process was applied in enhanced dispersion of CNT by introducing an organic cation which was a room-temperature ionic liquid (RILs) were found and upon being ground with CNT to form physical gels via cation-π interaction.[6,7] Whatever chemical modification or physisorption are utilized, the dispersion of CNT can be improved greatly.

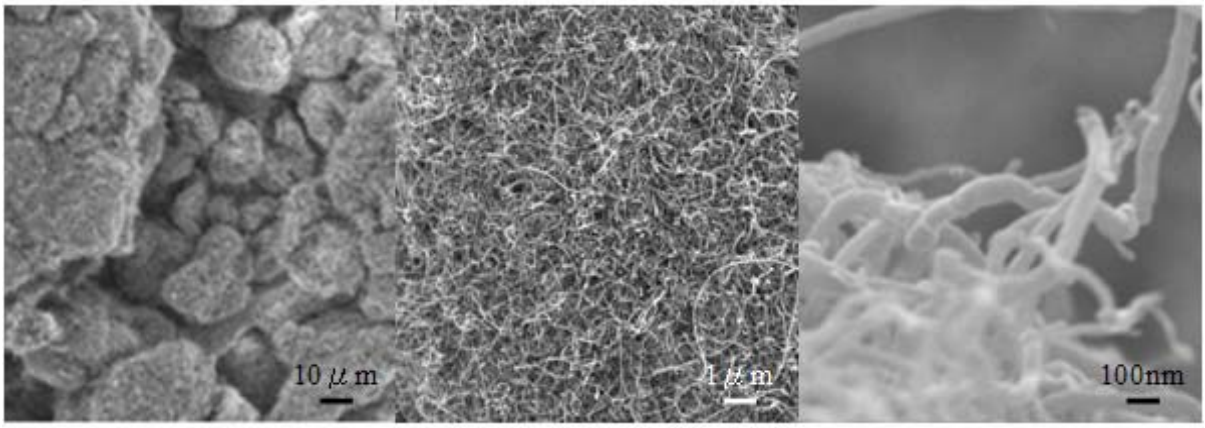

Figure 2. Entanglement of Carbon Nanotubes.

2. Overviews

2.1. Introduction of Carbon Nanotubes

2.1.1. Discovery of Carbon Nanotubes

The discovery of CNT can be traced back to the study of carbon clusters (fullerene). In the 1990s, the Royal Swedish Academy of Sciences has decided to award the 1996 Nobel Prize in Chemistry to Harold W. Kroto, Robert F. Curl and Richard E. Smalley for the discovery of fullerenes (Figure 3(a)),[8,9] which motivated a flurry of interest in exploring fullerenes. Among the studies of fullerenes, Iijima et al. were the most famous. In 1991, when they prepared C_{60} by arc-discharge method, they found long, thin cylinders of carbon by observation of high-resolution tunneling electron microscopy (HR-TEM) and they named it carbon nanotubes (Figure 3(b)).[10]

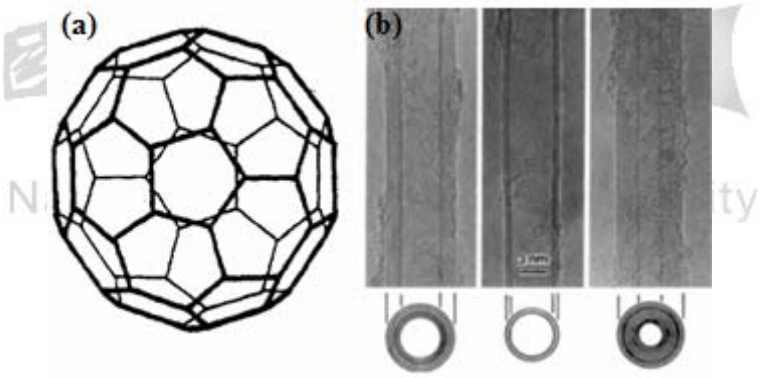

Figure 3. Discovery of (a) C_{60}[8,9], (b) Carbon nanotubes[10].

2.1.2. Synthesis of Carbon Nanotubes

In general, there are three ways for synthesizing CNT, arc discharge method, chemical vapor deposition (CVD) and laser ablation. Arc discharge method which created a vapor between end-to-end carbon electrodes with or without catalyst was reported by Ebbesen and Ajayan in 1992.[11] CVD which resulted in MWNT or poor quality of SWNT by placed substrate coated with catalyst (e.g. Fe, Co and Ni, etc.), heated to 600^{o}C and slowly feed a carbon gas (e.g. methane, etc) was reported by

Endo in 1993.[12] CNT, prepared from CVD, have a large diameter range, and it is a favored commercial production because of the easiness to scale up. In laser ablation technique, a high-power laser beam impinges on a volume of carbon-containing feedstock gas, which was reported by Smalley's group in 1995.[13] Both pulsed,[14,15] or continuous[16,17] laser beam were used to vaporize a graphite target in an oven filled with helium or argon gas at 1200°C. After expansion and cooling rapidly, carbon vapor condensed quickly and formed CNT.

2.1.3. Structure and Property of Carbon Nanotubes

The structure of CNT can be visualized by wrapping a one-atom-thin layer of graphite (called graphene) into a seamless cylinder. According to the number of graphite layer, there are two types of CNT, single-walled carbon nanotubes (SWNT, Figure 4(a)) and multi-walled carbon nanotubes (MWNT, Figure 4(b)). Both SWNT and MWNT can be classified by the chiral vector of graphite sheet (n,m), armchair type, zigzag type and chiral type (Figure 5).[18]

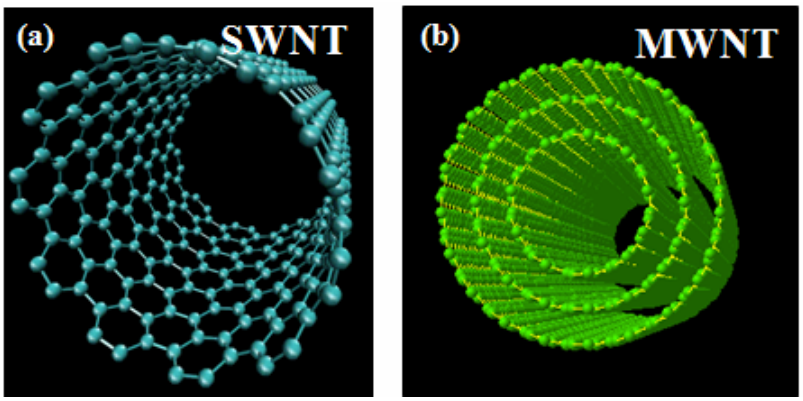

Figure 4. Structures of CNT: (a) SWNT and (b) MWNT.

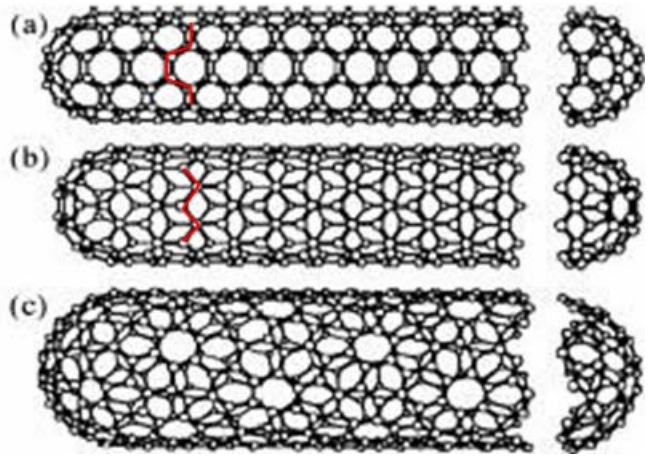

Figure 5. Structures of CNT: (a) armchair type, (b) zigzag type and (c) chiral type.[18]

CNT have exceptional physical and chemical properties due to high aspect ratio and a perfect structure of CNT which composed by sp^2 bond. The chemical reactivity of CNT is directly related to the pi-mismatch and the perfect seamless structures.[19,20] Similar to graphite and carbon black, CNT has extremely stable reactivity and excellent thermal stability. The electric property of CNT is strongly affected by the symmetry and unique electric structure of graphite sheet (n,m).[21,22] It was shown that CNT (n,m) with 2n+m=3q (where q is an integer), then CNT are metallic, otherwise the CNT are a semiconductor. In general, an armchair type (m=n) CNT are metallic, and a zigzag type (m=q, n=0) CNT are 1/3 metallic and 2/3 semiconductor (Figure 6).[23]

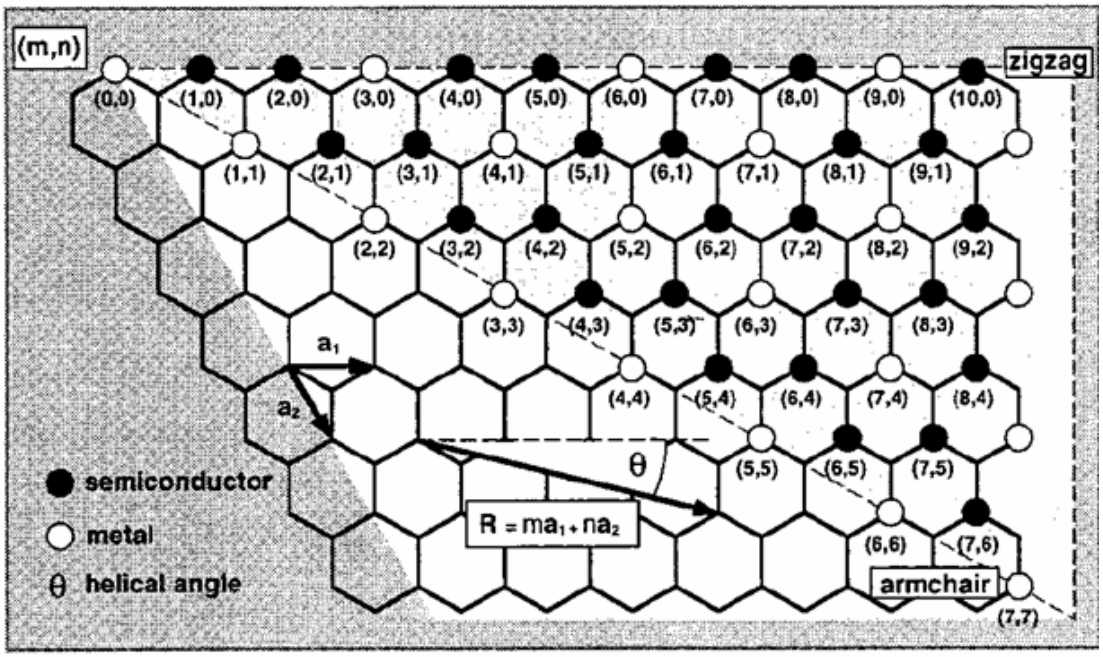

Figure 6. The relation between graphite sheet and electric property of CNT.[23]

Due to the seamless and graphite structure, CNT have excessive tensile, high compression and strong Young modulus in their axial direction. In general, the CNT tensile is better than the steel and strong as a diamond. In Yakobson`s research, the mechanical property of CNT is influenced by the dimension, curvature of CNT and ambient temperature.[24,25] CNT are brittle at high strain and low temperature, while at low strain and high temperature CNT can be completely or partially ductile.[26,27] CNT are expected to have excellent thermal conductivity due to the high crystalline and large photon mean free paths.[28,29] Compared to the grapheme and diamond, CNT have higher thermal conductivity. M. A. Osman et al. reported the thermal conductivity of CNT also is affected by the CNT dimension and ambient temperature. The CNT with large dimension have higher thermal conductivity.[30] In J. Hone et al. research, it showed the thermal conductivity is greatly depended on ambient temperature and significantly reduce with the increasing temperature at 100 K~400 K.[31,32,33]

2.2. Overview of Chemical Modification

CNT has various applications such as biochemical medicine,[34,35,36,37,38] nanocomposites,[39,40,41] electro-optical materials[42,43,44] and fuel development,[45,46] etc., and a vital step in developing the technology and manipulation of CNT is to take advantage of the rich chemistry. Up to the present, there are various chemical methods for CNT modification, including Bingel reaction (Figure 7(a)),[47] cyclo addition (Figure 7(b))[48] and anionic polymerization (Figure 7(c)),[49,50] etc. Among those chemical methods, strong oxidation is the most useful and studied widely (Figure 7(d) and (e)). Recently, both atom transfer radical polymerization (Figure 7(f)) and free radical polymerization (Figure 7(g)) also are applied in CNT modification.

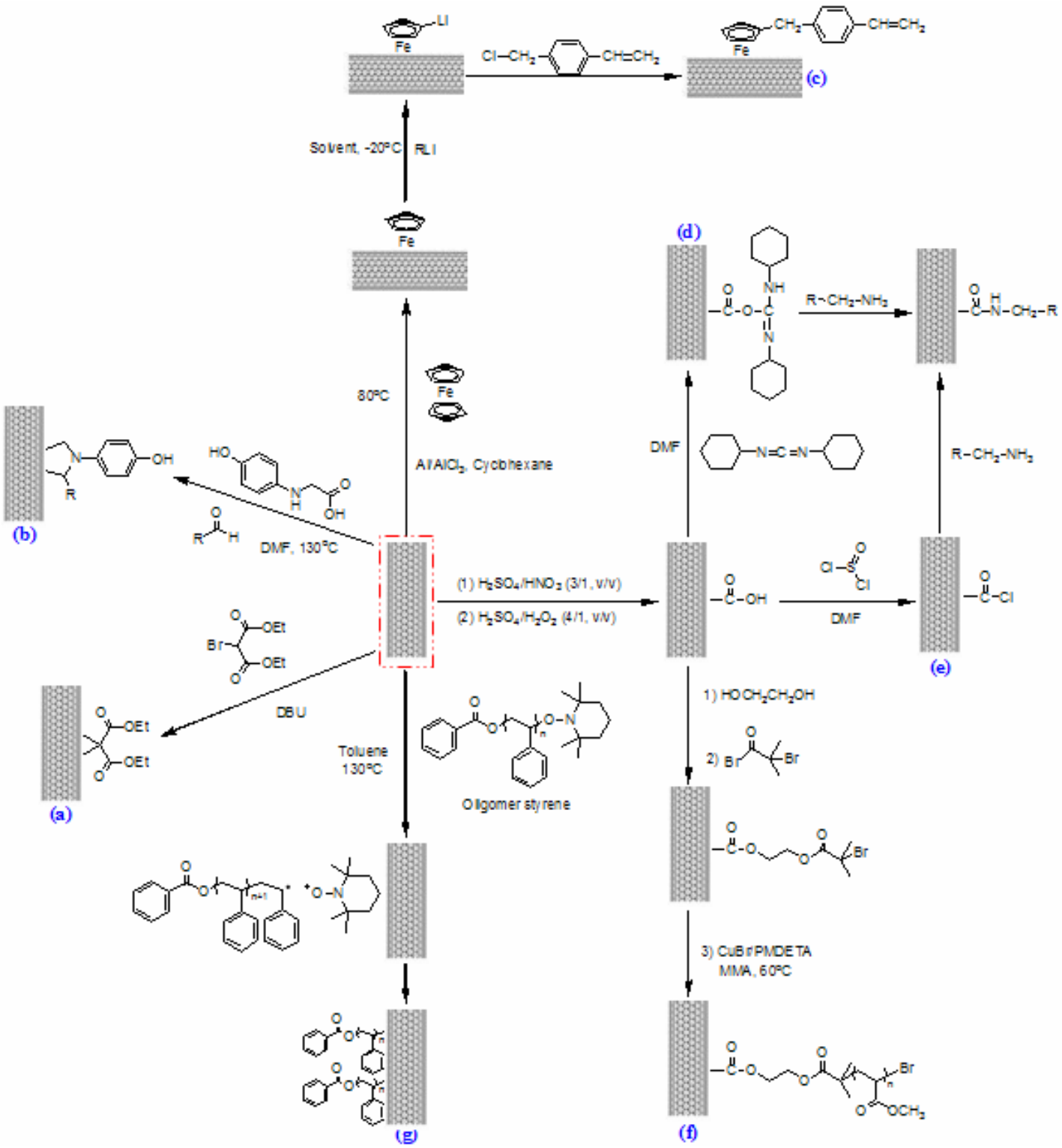

Figure 7. Chemical modification of CNT: (a) Bingel Reaction, (b) Cyclo Addition, (c) Anionic Polymerization, (d) DCC-activated Reaction, (e) Thionyl chloride-activated Reaction, (f) Atom Transfer Radical Polymerization, (g) Free Radical Polymerization.

2.2.1. Strong Oxidation

Taking advantage of the diversity of derivation, CNT can be modified and controlled via extremely chemical approaches such as strong oxidation which was first applied by R. E. Smalley et al.[51] CNT were functionalized by a 3:1 mixture of concentration H_2SO_4/HNO_3 and polished by a 4:1 mixture of concentration H_2SO_4/H_2O_2 at ambient temperature., which can form carboxylic acid groups on CNT surface. Those carboxylic acid groups can be activated by N', N'-Dicyclohexyl carbondiimide (DCC, Figure 7(d))[52,53,54] or thionyl chloride (Figure 7(e)),[55,56,57,58] etc., which can further react with alkylamine, alkyl alcohol, DNA or protein in order to improve the dispersion of CNT for various studies.

2.2.2. Free Radical Polymerization

CNT, composed of sp^2 bonds, can be functionalized via free radical reaction (Figure 7(g)).[59,60] In W. T. Ford et al. researches, CNT can be modified by styrene successfully via free radical polymerization.[61] Taking the synthetic method using a free radical polymerization, the modified CNTs maintain their reactivity for reaction and enable to reserve the growing polymer radical chain end.

2.2.3. Atom Transfer Radical Polymerization (ATRP)

Recently, ATRP also was applied in modification of CNT. In W. Ford[62,63] and C. Gao et al.[64,65,66] research, CNT were functionalized by H_2SO_4/HNO_3 and activated by thionyl chloride first and then alkyl halide grafted from the functionalized CNT. Finally, alkyl halide-graft-CNT reacted with styrene monomer (or methyl methacrylate monomer) and metal complex ligand via ATRP (Figure 7(f)). Compared to free radical polymerization, ATRP is more controllable and also has low polydispersity.

2.3. Overview of Physisorption

Although CNT can be fabricated by various chemical reactions and have been used to achieve effective dispersion, it has found that those chemical techniques will deteriorate the intrinsic properties of CNT. Physisorption which is an alternative has proven capable of de-bundling CNT bundles and stabilizing individual tubes while maintaining the CNT integrity and intrinsic properties. Two steps are involved with physisorption---physical dispersion and mediate adsorption. The former, for example ultrasonication, roll miller and screw-extruder, is used to redistribute van der Waals bonding force among the CNT molecules. The latter, for instance surfactants, polymers and protein, is used to disperse and prevent from flocculation of CNT bundles.

2.3.1. Surfactants

Due to interaction between CNT and amine moiety, surfactants which contain amine group are utilized for CNT dispersion.[67,68,69] The major mechanism of interaction between CNT and amine moiety is charge transfer.[70,71,72,73] In addition, surfactants with aromatic moieties, polar groups and alkyl segments are enable CNT to adsorb more surfactants. In R. E. Smalley et al. researches,[74] for the ionic surfactant, sodium dodecylbenzene sulfonate (SDBS) gives the best dispersion of CNT (20 mg/ml) and for nonionic systems, surfactants with higher molecular weight suspend more CNT materials. I. J. Chung et al. reported surfactants with a lipophilic group equal to and longer than decyl, containing 9 methylene groups and 1 methyl group, contribute to the dispersion of CNT in water.[75]

2.3.2. Polymers

A supra-molecular approaches, polymer wrap, were applied in dispersion of CNT via hydrophobic force or π-π stacking.[76,77,78,79,80,81] Polymers contain rich aromatic moieties are the best candidate, for example polystyrene[82,83] and conducting polymer[84,85,86,87,88], etc. Taking advantage of chemistry, polymers can be prepared and tailored by chemical technique and be able to organize CNT into ordered network or self assembly.[89]

2.3.3. Proteins

Applications in biology, for example biosensor, protein immobilization and bio-electronic nano-materials, are great interest for scientists. The high conformational compatibility of CNT and proteins, which are driven from unique geometry and hydrophobic effect between CNT and proteins make CNT possible to apply in biology (Figure 8). In the early research, streptavidin[90,91] and metallothionein[92,93,94,95] were chosen to study the interaction between proteins and CNT. It was found that CNT can strongly interactwith proteins and can almost completely be covered by proteins due to the rich hydrophobic segments on proteins. Recently, G. R. Dieckmann and H. Musselman co-worked and designed a protein contain a peptide which is enable to fold into an amphiphilic α-helix.[96,97,98] The hydrophobic and hydrophilic segments of the helix were intended to interact non-covalently with the aromatic surface of CNT and self assembly through hydrogen bonds.

3. Materials, Experimental and Instruments

In my thesis, a new approach of CNT dispersion was developed by grinding layer silicates, synthetic mica (Mica), with CNT and enhanced dispersion of CNT remarkably in both hydrophobic and hydrophilic solvents. The other clays including sodium montmorillonite (MMT) and layer double hydroxides (LDH) were examined. All hybrids were prepared, examined and discussed as follows. Sequentially, a series of polyvinyl acetate composites were prepared and measured.

3.1. Materials

(a) Multi-walled carbon nanotubes (MWNT)

MWNT was supplied by Seedchem Company Pty., Ltd. and prepared from chemical vapor deposition (CVD). The carbon nanotubes are 95% in purity, average 40~60 nm in diameter and 0.5~10 μm in length.

(b) Synthetic fluorinated mica (Mica)

The synthetic fluorinated mica (SOMASIF ME-100), with a chemical composition of Si (26.5 wt %), Mg (15.6 wt %), Al (0.2 wt %), Na (4.1 wt %), Fe (0.1 wt %), and F (8.8 wt %) was obtained from CO-OP Chemical Co. (Japan). The geometric structures of the pristine Mica are irregularly aggregated from the primary units consisting of silicate platelets in stacks. The unit platelets are irregularly shaped and ionic charges with $SiO^{-}Na^{+}$. Their average dimension was estimated to be $300\times300\times1$ nm^3.[99] Due to the presence of intensive ionic charge character, these clays are capable of swelling in water and gelling at high concentration. Their interlayer space between the neighboring platelets is commonly 1.2 nm *d* spacing (by XRD measurement in dried powder).[100] These silicate/aluminum oxide layers are filled with exchangeable cationic metal counter ions,[101] titrated to be 1.2 mequiv/g.

(c) Sodium montmorillonite (MMT)

Sodium montmorillonite was supplied from Nanocor Co. The geometric structures of the pristine MMT are irregularly aggregated from the primary units consisting of silicate platelets in stacks. The unit platelets are irregularly shaped and ionic charges with SiO^-Na^+. Their average dimension was estimated to be 100×100×1 nm^3.[106] Due to the presence of intensive ionic charge characters, these clays are capable of swelling in water and gelling at high concentration. Their interlayer space between the neighboring platelets is commonly 1.2 nm *d* spacing (by XRD measurement in dried powder).[107] These silicate/aluminum oxide layers are filled with exchangeable cationic metal counter ions,[108] titrated to be 1.2 mequiv/g.

(d) $AlMgO_x^-NO_3^-$ layered double hydroxide (LDH)

LDH were prepared by a co-precipitation process according to the previously reported procedures.[102] A mixture of $Mg(NO_3)_2{\cdot}6H_2O$ (120 g, 0.48 mol) and $Al(NO_3)_3{\cdot}9H_2O$ (90 g, 0.24 mol) was dissolved in 1-liter deionized water (the Mg/Al molar ratio was 2.0). The aqueous solution was vigorously stirred at 60°C under nitrogen purge in order to minimize contamination with atmospheric CO_2. The pH was maintained at 10 ± 0.2 by portion-wise addition of 4 N NaOH. The resulting suspension was stirred at 60°C for 16 h. The white precipitate was isolated by filtration and washed thoroughly with deionized water. The X-ray diffraction (XRD) showed a basal spacing of 7.8 Å. The clays have average dimension LDH (200×200×1 nm^3).

(e) Polyvinyl Acetate (PVA)

Polyvinyl alcohol which was supplied by Aldrich Co. was 98~99% hydrolyzed with a molecular weight ca 83000. Solutions of PVA was made stirring appreciate quantities of PVA and deionized water at > 90°C for at least 3 hours.

(f) Solvents

Solvents such as ethanol, isopropyl alcohol (IPA), acetone, 2-butone (MEK), tetrahydrofuran (THF), toluene, dimethyl formamaide (DMF) and dimethyl aceticamide (DMAC) were used as received. Deionized water (18.2 MQ) was produced by a Millipore Milli-Q Plus Ultra Pure Water system.

3.2. Experimental

A. New Method of Dispersing MWNT

All experiments were described as below:

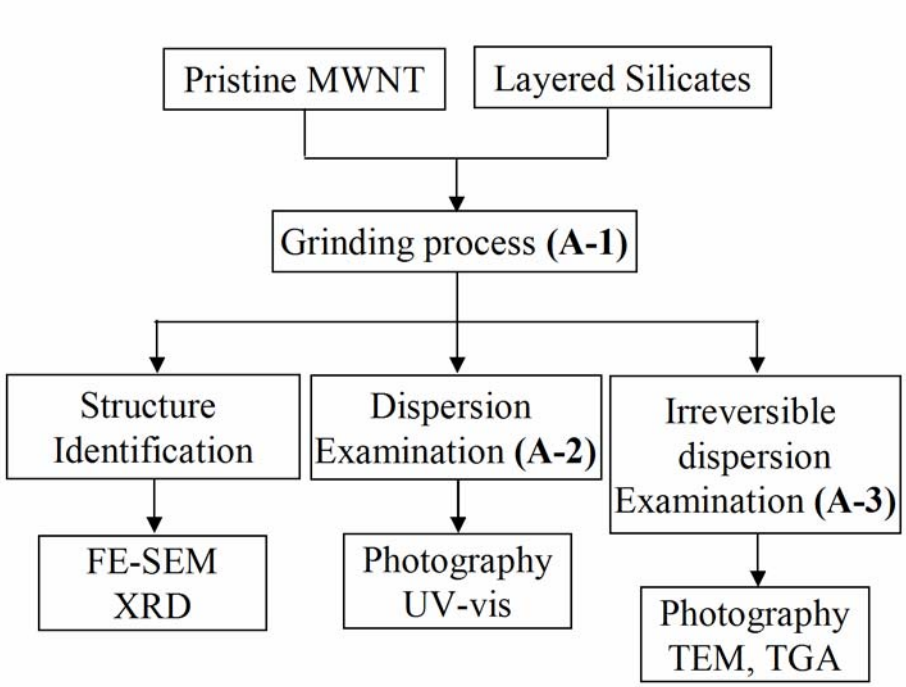

A-1 Preparation of MWNT-Clay Hybrid

The procedure of preparing MWNT-Mica hybrid (MMH) is exemplified below. MWNT (0.06 g) and Mica (0.06 g) were ground adequately in an agate mortar and pestle. The sides of the mortar were occasionally scraped down with the pestle during grinding to ensure a thorough mixing. The mixture was washed from mortar and pestle using deionized water at concentration of 1 mg MWNT/20 g water. The MWNT-Mica hybrid were prepared at weight ratios, clay/MWNT or α ratio = 0.33, 0.5, 1, 2 and 3. MWNT-MMT hybrid and MWNT-LDH hybrid were prepared as same procedure described above. MWNT-MMT hybrid (MTH) were prepared at α = 1, 2, 3, 4, 5, 6 and 7. MWNT-LDH hybrid (MLH) were prepared at α = 1, 2, 3, 5 and 7.

A-2 Dispersion of MWNT-Clay hybrids in solvents

Different weight ratios of MWNT-Clay were dispersed in 20 g deionized water by shaker or ultrasonication. All hybrids were dispersed in water at various concentrations (1×10^{-3}~5×10^{-3} wt %). The suspension of MWNT-Mica hybrid was heated (20~80^{o}C) by a hot plane with magnetic stirrer and then analyzed by UV-vis spectrometer. The dispersion of MWNT-Mica hybrid in common solvents and the control experiments were exemplified below. Mica (2 mg), MWNT (1 mg) and MWNT-Mica hybrid (3 mg at α=2) respectively dispersed in 20 g solvents such as water, ethanol, IPA, acetone, MEK, THF, toluene, DMF and DMAC by a shaker or ultrasonication (BRANSON 5510R-DTH 40 Hz) for 2 min

A-3 Amphiphilic Property and Irreversible Dispersion of MWNT-Mica hybrid

Ternary mixtures of the MWNT-Mica hybrid were examined for the dispersion ability in water and toluene in different order of addition. In the first example, the hybrid of CNT-Mica (3 mg at α = 2) was dispersed in 7.5 g water first, thoroughly dispersed and then added with 7.5 g toluene. I example, the hybrid was dispersed in toluene, homogeneous mixed and then added with water. During the mixing, ultrasonic vibration was applied.

B. PVA Nanocomposites

Preparation of Mica-PVA, MWNT-PVA and Hybrid-PVA composites were described as below.

Method I

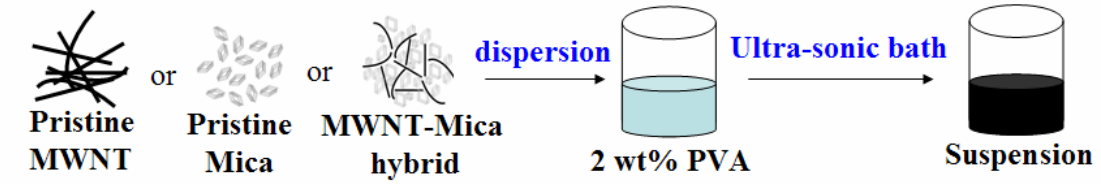

Method II

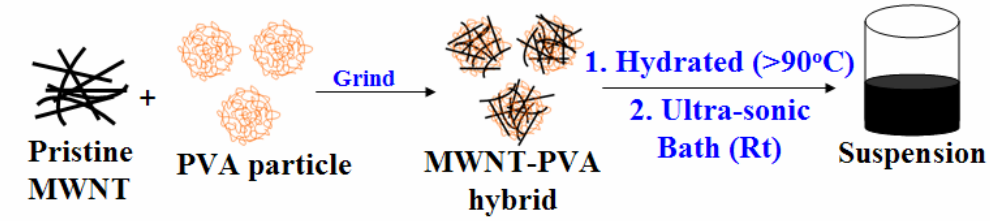

Method I.

Mica powder, pristine Mica and MWNT-Mica hybrid (α = 2) powder was dispersed in PVA solution (2 wt %) by ultrasonication (BRANSON 5510R-DTH 40 Hz) for 2 min. All suspensions were heated by an oven at 80°C for 3 hours and then dehydrated by an oven at 80°C for 2 hours. Hybrid-PVA composites were prepared at hybrid/PVA weight fractions of 1.5, 3, 9 and 15 wt%. Mica-PVA composites were prepared at Mica/PVA weight fraction of 1, 2, 4, 6 and 15 wt%. MWNT-PVA composite was prepared at MWNT/PVA weight fraction of 0.5 wt%.

Method II.

Pristine MWNT powder was pulverized with PVA powder in an agate mortar and pestle. The sides of the mortar were occasionally scraped down with the pestle during grinding to ensure a thorough mixing. All hybrids were dissolved in deionized water at > 90°C for at least 3 hours and then dehydrated by an oven at 80°C for 2 hours. MWNT-PVA composites were prepared at MWNT/PVA weight ratios of 0.5, 1, 3, 5 and 15 wt%.

3.3. Instruments

(a) Ultraviolet-visible Spectrometer (UV-vis)

The dispersions of MWNT-Mica hybrid in deionized water were analyzed by using an optical absorption at 550 nm on a Perkin-Elmer Lambda 20 UV–vis spectrophotometer. Variables of concentration, temperature and time are taken into account and discussion.

(b) Thermal Gravimetric Analyzer (TGA)

First, samples were dried in a vacuum for 24 h at 120^{o}C. After dehydration, 3~8 mg sample was placed at platonic pan and then the pan was sent into TGA furnace. TGA was performed by using a Perkin Elmer Pyris 1, with a temperature gradient that ramped from 100 to 800^{o}C at a rate of 10^{o}C/min.

(c) X-ray Diffraction (XRD)

First, samples were coated on a glass substrate and then dehydrated in a vacuum for 24 h at 120^{o}C. XRD was recorded on a Schimadzu SD-D1 diffractometer with Cu target (k =1.5405 Å) at a scan rate of 2^{o}/min (θ>2^{o}). The basal spacing (n=1) was calculated according to Bragg's equation ($n\lambda=2d\sin\theta$) through the observed peaks of n=2, 3, etc.

(d) Field-Emitting Scanning Electron Microscopy (FE-SEM)

First, samples were dehydrated in a vacuum for 24 h at 120^{o}C and then adhered by carbon tape. Finally, Au coating was carried out for the samples before the FE-SEM measurements. FE-SEM images were obtained from a JEOL JSM-6700F SEM system.

(e) Transmission Electron Microscopy (TEM)

MMH which were suspended in deionized water or toluene at 0.01 wt% was dropped onto a carbon-coated copper grid and dried at ambient temperature. TEM was performed on a Zeiss EM 902A operated at 120 kV.

4. Results and Discussion

4.1. Preparation of MWNT-Mica hybrid

According to the geometric conception, we developed a convenient method for MWNT to directly disperse in water. An inorganic material, silicate platelet, which have large difference of geometric shape from tube shape of MWNT are enable to redistribute the van der Waals attractions between MWNT molecules through grinding method. Dispersions which are involved with difference of geometric shape are named *geometric shape dispersion* (Figure 9).

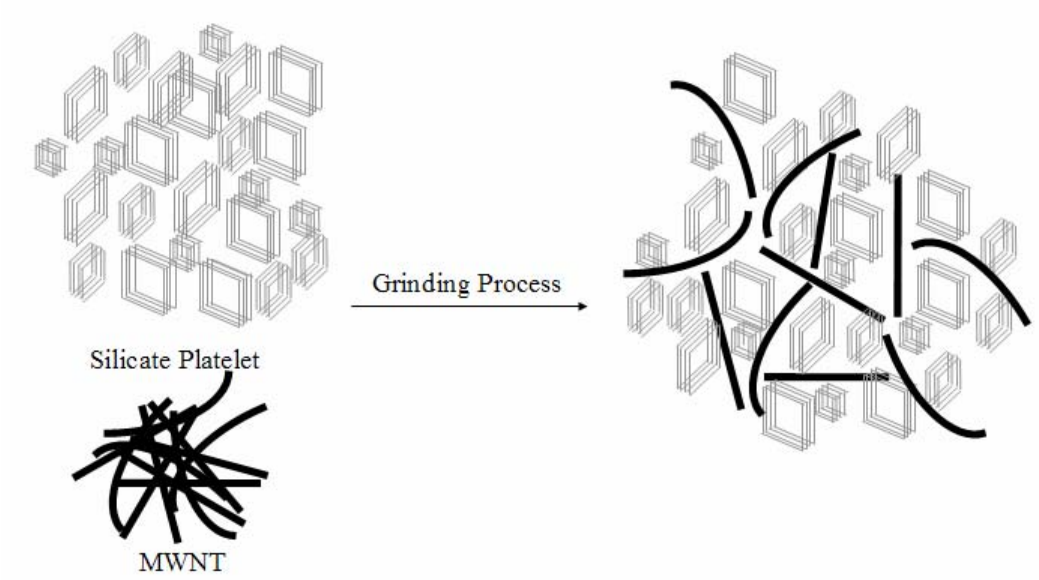

Figure 9. Conceptual Representation of Geometric shape dispersion

As described above in the experimental section, MWNT-Mica hybrid were prepared by grinding MWNT with Mica at weight ratios, α = Mica/MWNT = 0.33, 0.5, 1, 2, 3. The resultants were investigated by FE-SEM and XRD. In the observations of FE-SEM, it showed that MWNT and Mica were mixed completely and became almost homogeneous (Figure 10).

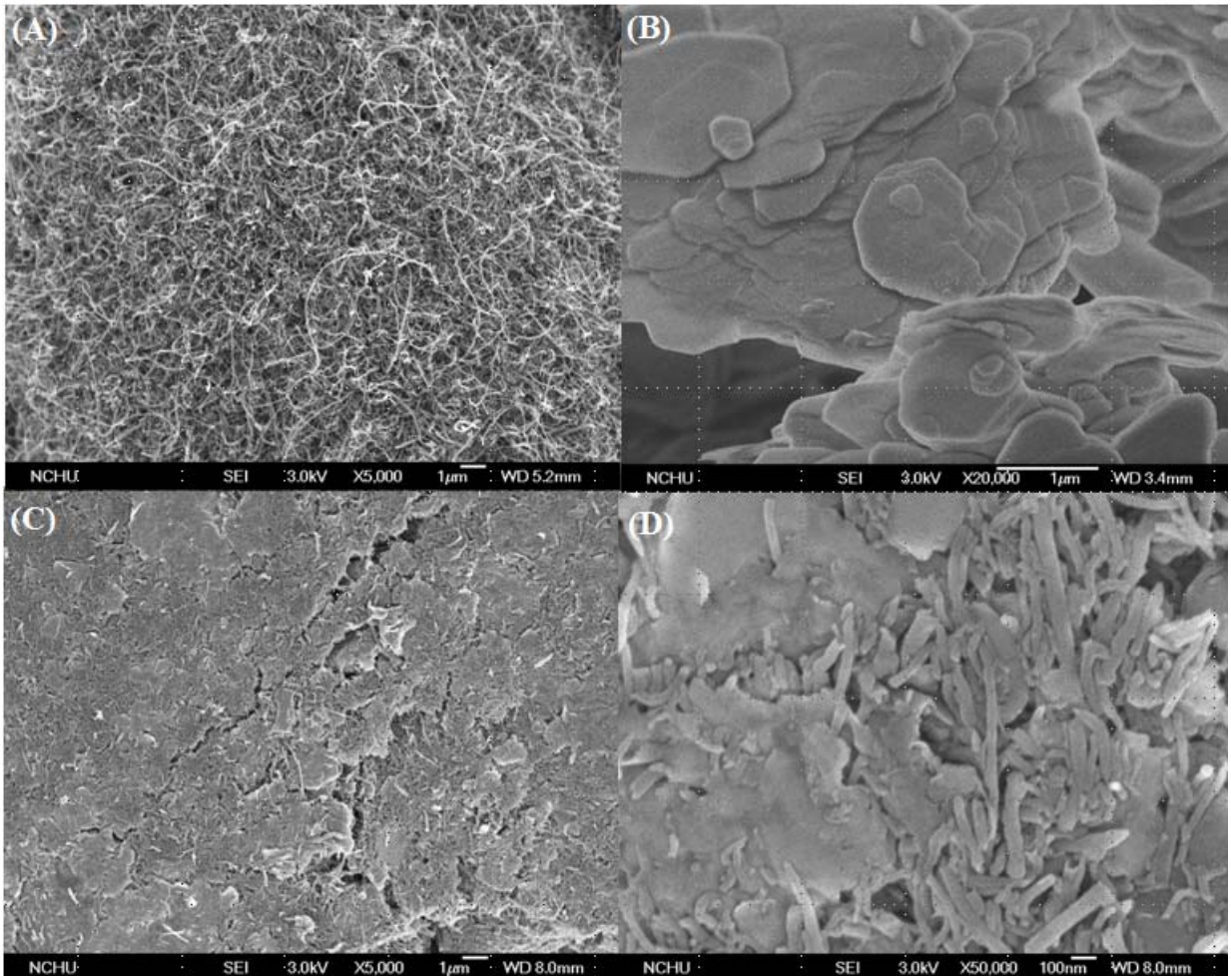

Figure 10. FE-SEM morphology of (A) pristine MWNT, (B) pristine Mica, (C) and (D) MWNT-Mica hybrid (α =2).

MWNT-Mica hybrid were examined by XRD in order to examined the layered structures of Mica were not destroyed by MWNT or grinding process. The results showed that the feature peak of Mica appeared at 2θ = 7.1 and d-spacing was 12 Å, indicated that the layer structures of Mica still maintain (Figure 11(A) and (B)). Due to the increase of Mica weight amount to hybrids, the following intensity of various MWNT-Mica hybrids was observed: MWNT-Mica hybrids (α = 3) > MWNT-Mica hybrids (α = 2) > MWNT-Mica hybrids (α = 1) > MWNT-Mica hybrids (α = 0.5) > MWNT-Mica hybrids (α = 0.33).

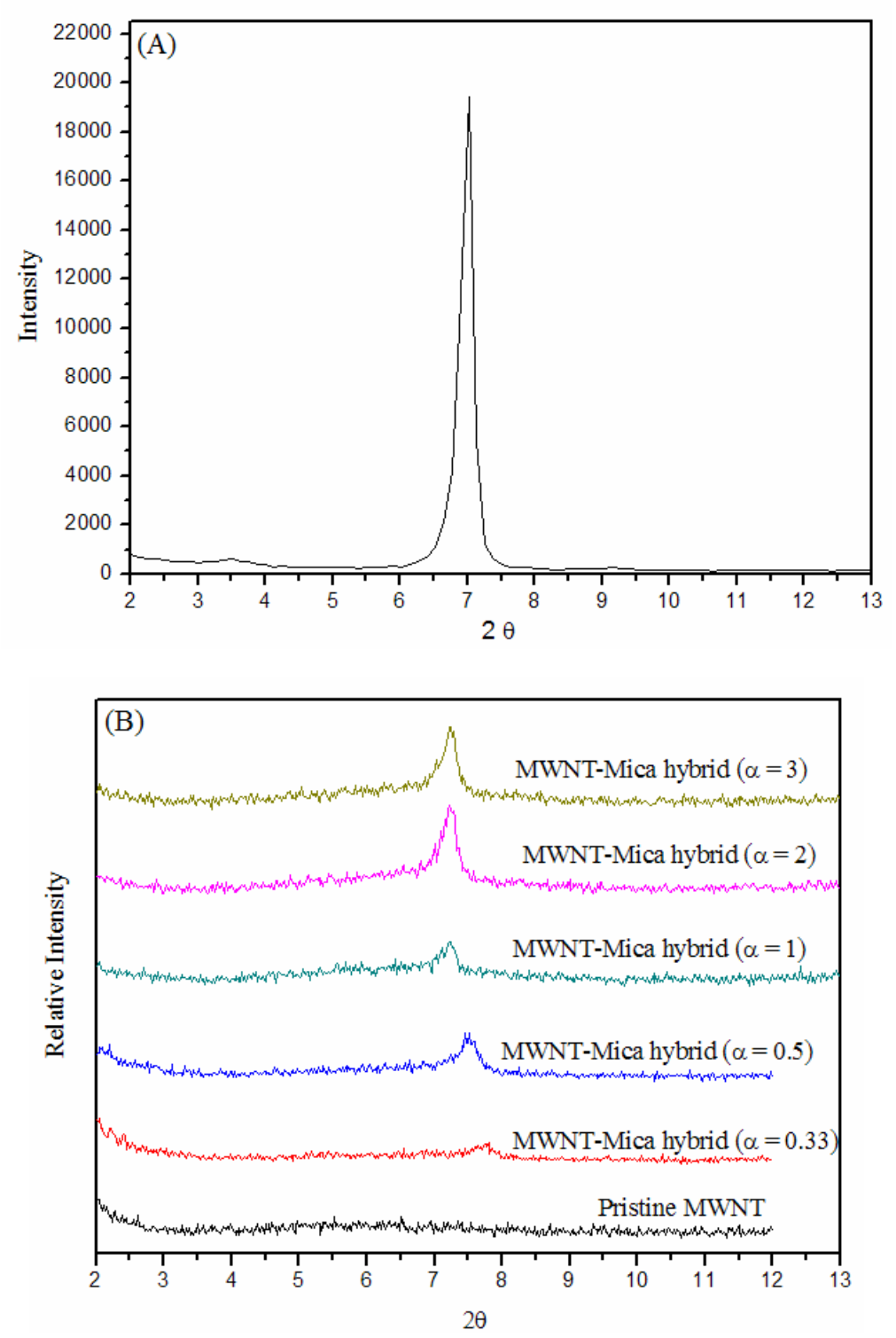

Figure 11. XRD of pristine Mica (A) and MWNT-Mica hybrids (B).

4.2. Dispersion of MWNT-clay hybrids in Water

The CNTs are in tubular shape and constituted of all conjugate sp^2 orbital bonds. Due to the high aspect-ratio dimension of 40~60 nm in diameter and 0.5~10 μm in length, the materials are easily aggregate and difficult to disperse in common organic solvents. The aggregation is mainly cause by the same nanoparticle van der Waals force attraction. However, when MWNT were ground with the inorganic clays, particularly the large platelet mica, their aggregation forces are minimized. The nanotubes were finely dispersed in a homogeneous manner. Initially, it was found that the MWNT-Mica mixtures at more than 1:1 weight ratio or $\alpha \geq 1$ could be easily dispersed into deionized water. As shown in Figure 12, it is visually observed that the black CNT dispersed homogeneously in water when the MWNT-Mica ratios are more than one. With increasing MWNT amounts or decreasing the use of Mica, the effectiveness of dispersion significantly diminished. For example, at the hybrid of $\alpha <$ 0.5, the black MWNT are mostly precipitated at the bottom of bottle.

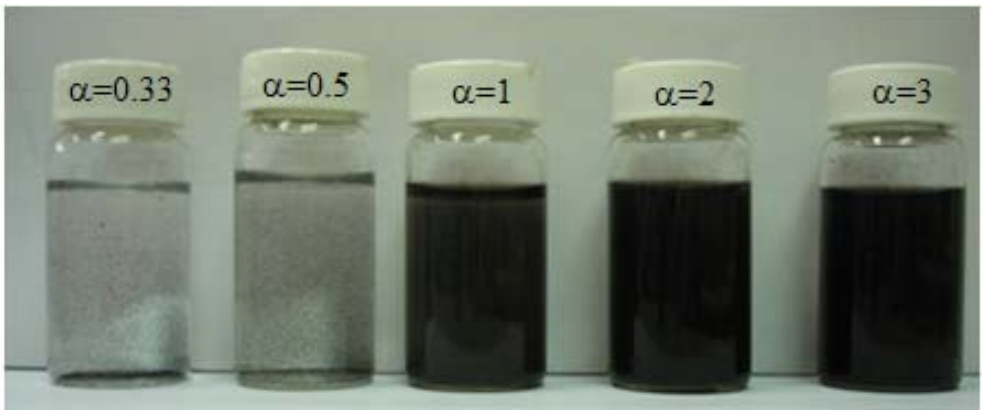

Figure 12. Visual observation of MWNT-Mica hybrids dispersion in water. (1 mg MWNT/20 g water; α = weight ratio of clay over MWNT in the ground hybrids)

The dispersant ability was further confirmed by analyzing the suspension by using a UV-visible spectrometry. In Figure 13, the relative absorption at 550 nm increases with the increasing weight amount of Mica addition to the hybrids, indicating the MWNT dispersion in water.[103, 104] The increase has reached a maximum for the ratio of MWNT-Mica approaching α = 2-3. The result implies the Mica has played a role for affecting the CNT dispersion but the effectiveness may have a limitation. It is visualized that the pristine tubular aggregation has been minimized but replaced by the interaction between CNT and Mica.

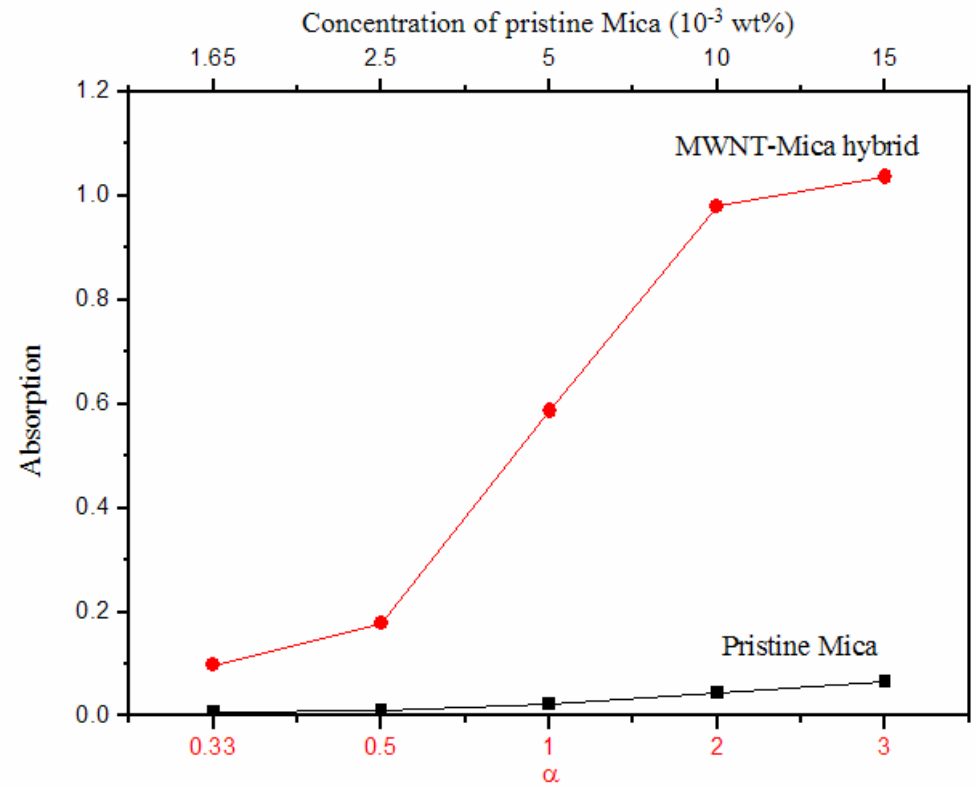

Figure 13. UV-vis spectra absorption of various weight ratios of MWNT-Mica hybrids and pristine clay dispersed in water. (1 mg MWNT/20 g water; α = weight ratio of clay over MWNT in the ground hybrids)

The dispersion solution of MWNT-Mica hybrid (α=2) was separated into several portions and diluted to different concentration, and their absorption spectra were measured (Figure 14). The absorption spectra were dependent on the solution concentration of MWNT-Mica hybrid (α=2) in a linear fashion and following the Lambert-Beer's Law.

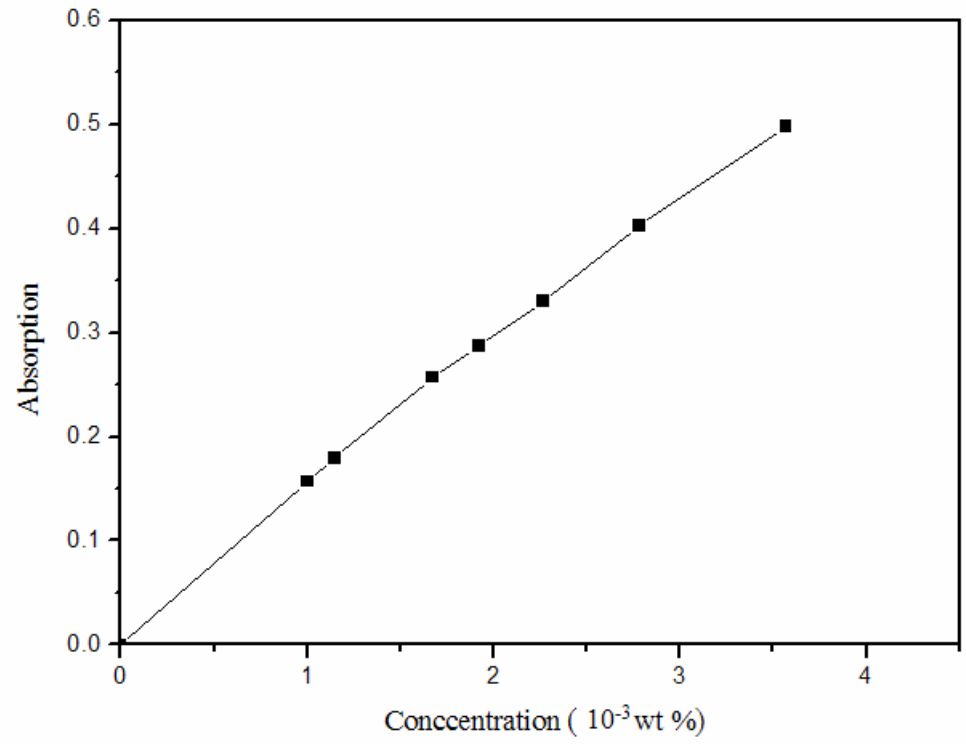

Figure 14. UV-vis absorption of MWNT-Mica hybrid (α = 2) in water with different concentrations.

In order to understand the nature of MWNT-Mica interaction, two other clays including montmorillonite (MMT) and layered double hydroxide (LDH) were examined. The clays with different average dimension, MMT ($100\times100\times1$ nm^3) and LDH ($200\times200\times1$ nm^3), were compared with Mica ($300\times300\times1$ nm^3) for their ability of rendering MWNT dispersion. MWNT-MMT and MWNT-LDH hybrids were prepared by using the same approach as described previously and all suspensions of the two hybrids rendered the same manner as dispersion behavior of MWNT-Mica hybrid (Figure 15(A) and (B)). The MWNT-MMT and MWNT-LDH mixtures at $\alpha \geq 3$ and $\alpha \geq 2$, respectively, could be easily dispersed into deionized water.

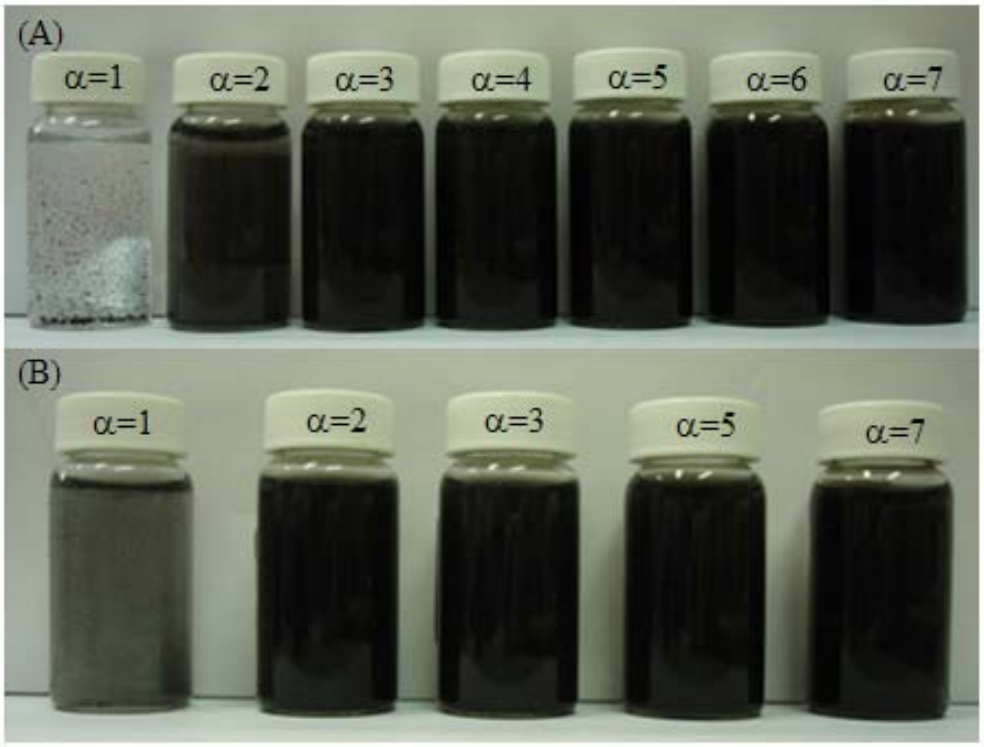

Figure 15. Visual observation of MWNT-clay hybrids dispersion in water: (A) MWNT-MMT hybrids and (B) MWNT-LDH hybrids. (1 mg MWNT/20 g water; α = weight ratio of clay over MWNT in the ground hybrids)

The dispersant ability was further confirmed by a UV-visible spectrometry. In Figure 16 and Figure 17, the relative absorption at 550 nm increases with the increasing weight amount of MMT and LDH addition to the hybrids, indicating the MWNT dispersion in water.[110,111] The increase has reached a maximum at the ratio approaching α = 6-7 for MWNT-MMT and α = 2-3 for MWNT-LDH. The absorption of MWNT-MMT and MWNT-LDH hybrids is also depended on the solution concentration in a linear manner, following the Lambert-Beer's law (Figure 18).

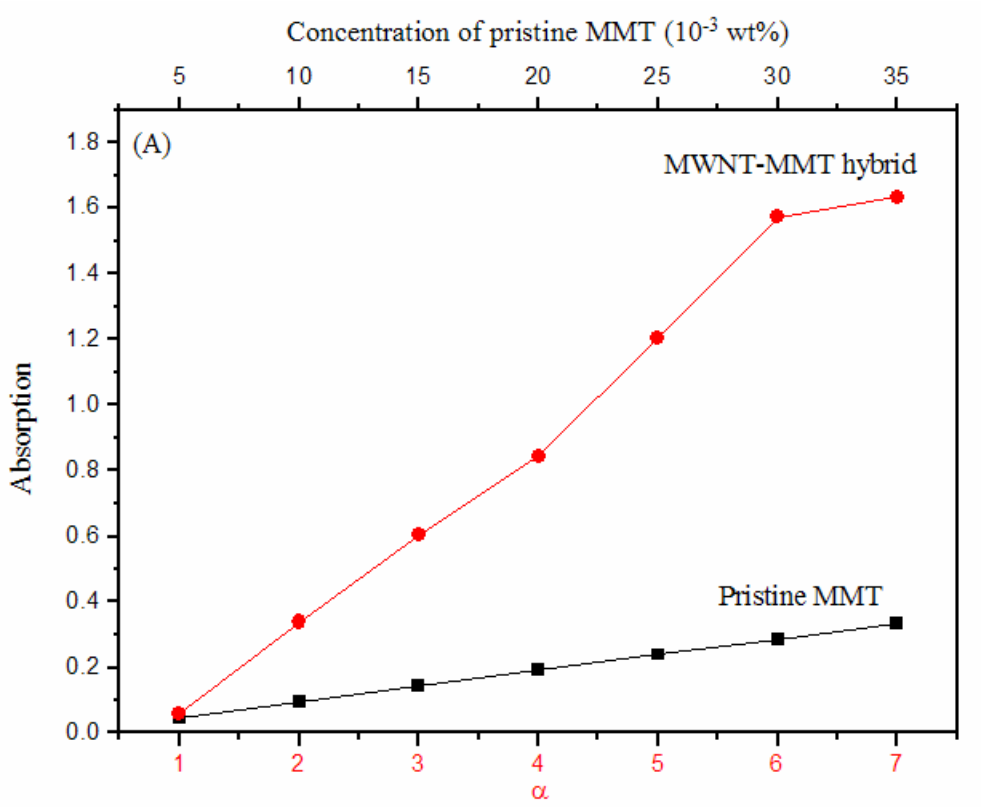

Figure 16. UV-vis spectra absorption of various weight ratios of MWNT-MMT hybrids and pristine clay dispersed in water. (1 mg MWNT/20 g water; α = weight ratio of clay over MWNT in the ground hybrids)

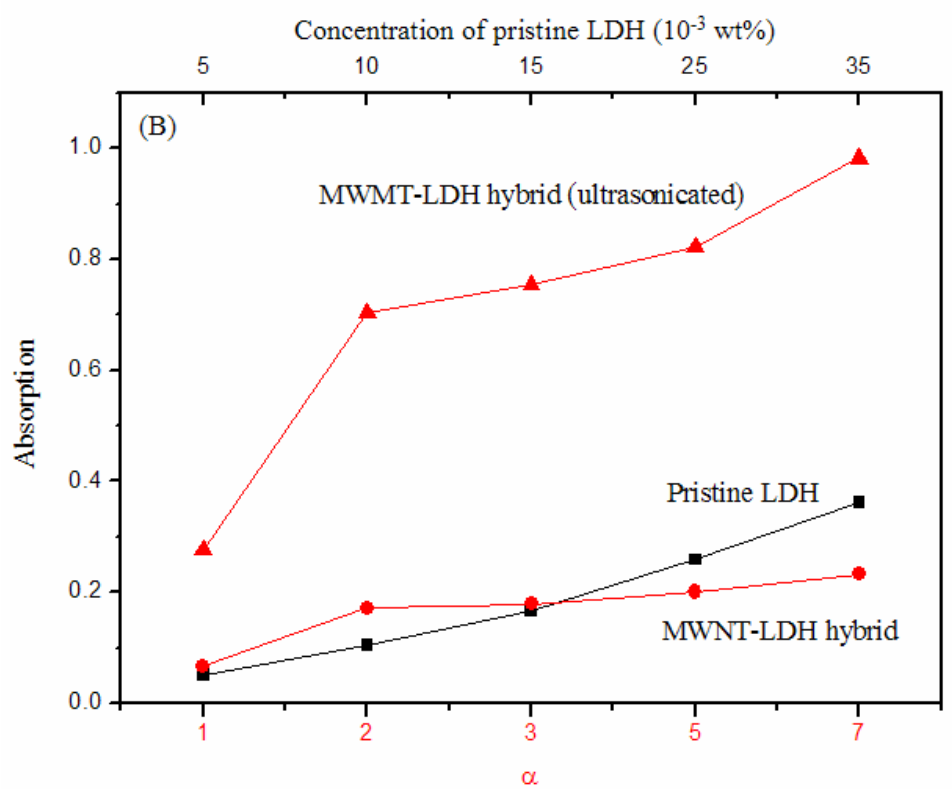

Figure 17. UV-vis spectra absorption of various weight ratios of MWNT-LDH hybrids and pristine clay dispersed in water. (1 mg MWNT/20 g water; α = weight ratio of clay over MWNT in the ground hybrids)

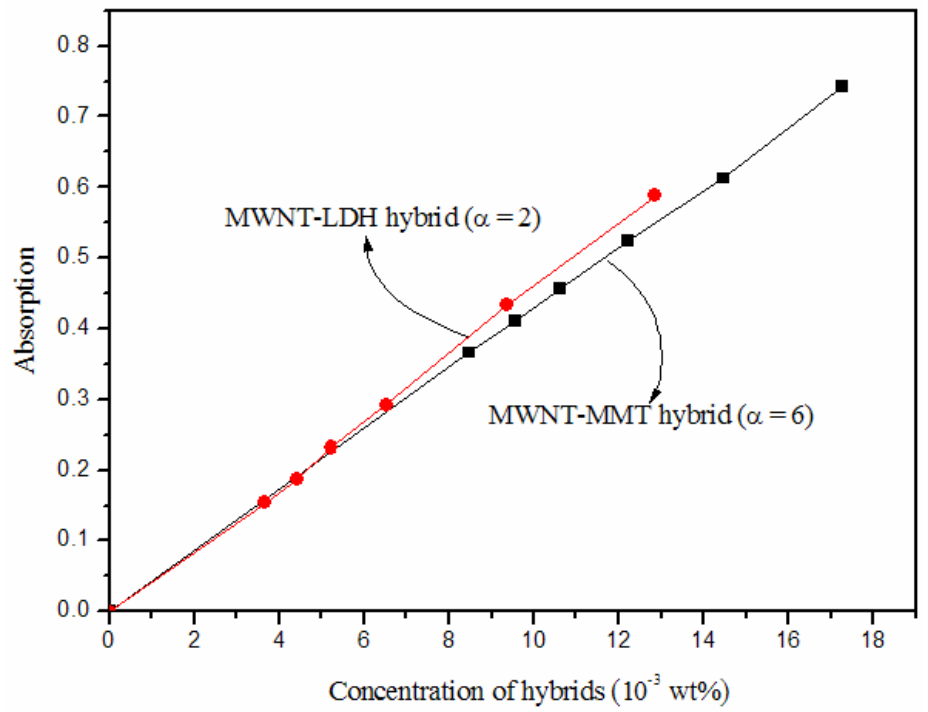

Figure 18. The linear dependence of the absorption at 550 nm on concentration of MWNT-MMT (α=6) and MWNT-LDH hybrid (α=2).

On the basis of UV-vis analysis (Figure 19), the Mica is the most effective clay perhaps due to its high aspect ratio and difference from the MWNT geometric shape (Figure 20). In view of their ionic charges, the LDH is anionic clays consisting of surface cationic charges and nitrate anionic species as the counter ions. The opposite charge distribution on the clay surface (SiO^-Na^+ for MMT and Mica) may be the second reason for the lower ability of interacting with MWNT (Figure 21). It seems that the advantage of Mica shape difference from MWNT is the most effective factor for controlling the MWNT dispersion in water.

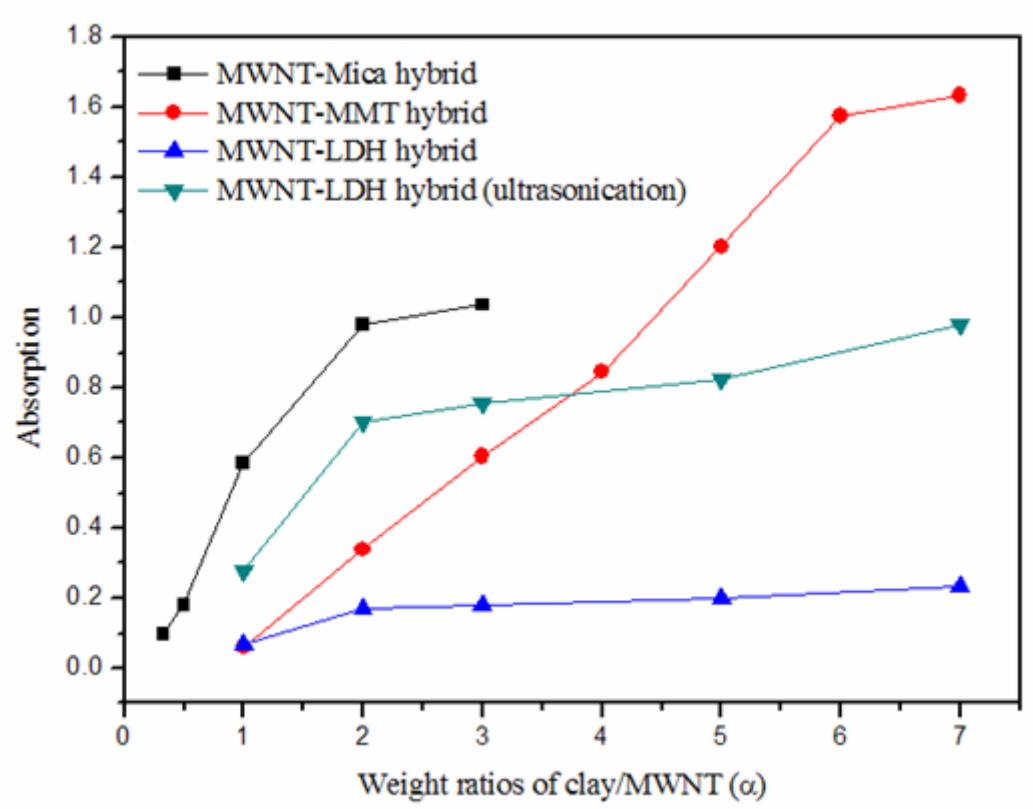

Figure 19. UV-vis spectra absorption of various weight ratios of MWNT-clay hybrids dispersed in water. (1 mg MWNT/20 g water)

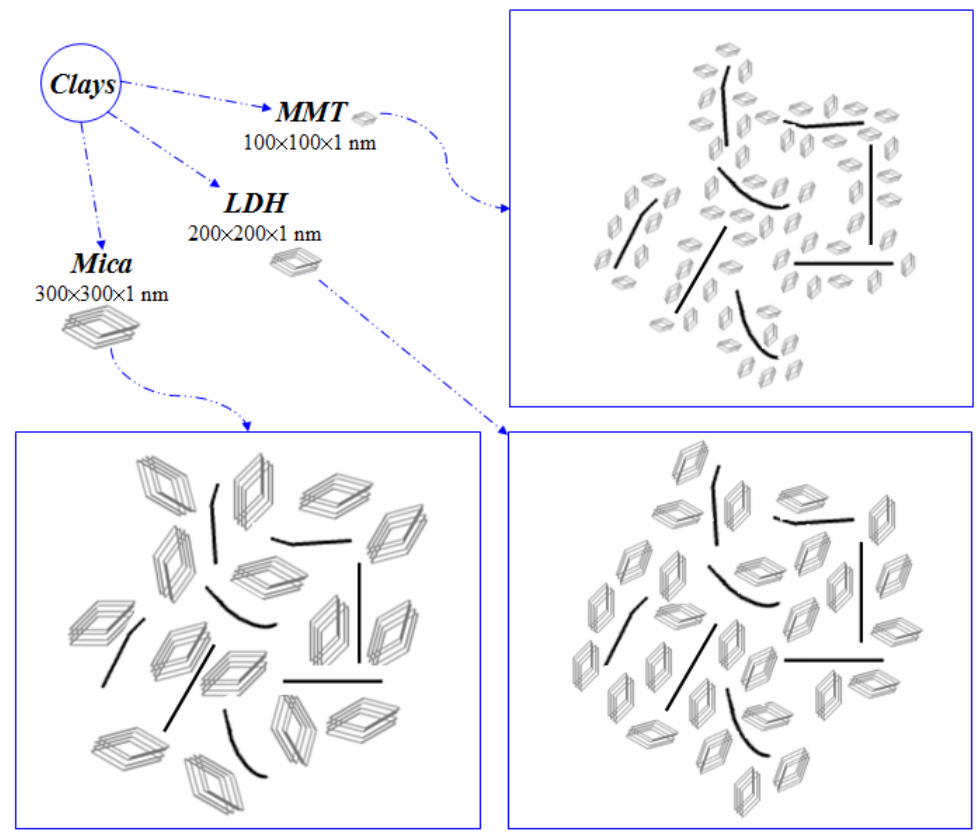

Figure 20. Aspect ratio factor influenced on dispersion.

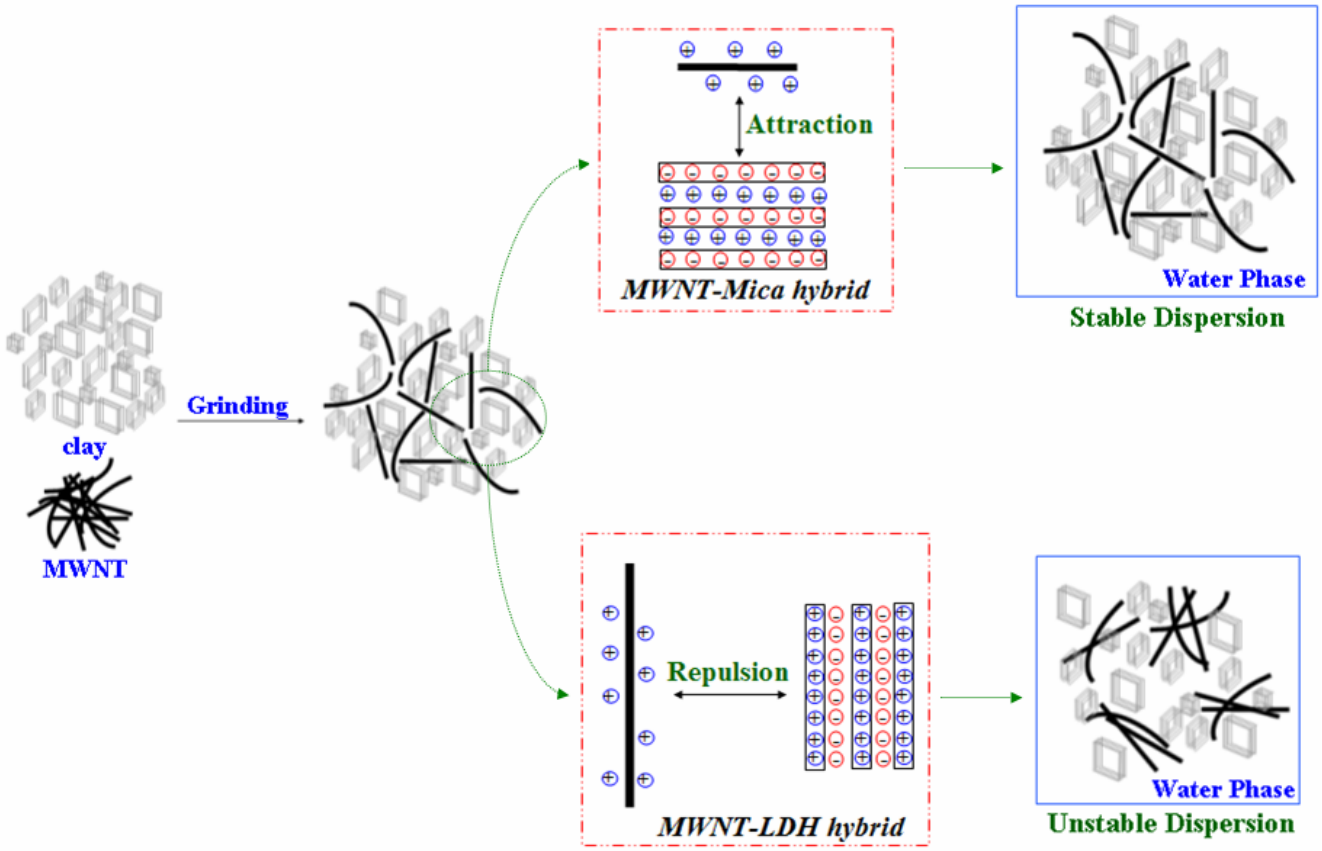

Figure 21. Surface charge factor influenced on dispersion.

4.3. Stability of suspension and Influence of Temperature on MWNT Dispersion

Compared to other clays, Mica is the most effective clay for MWNT dispersion due to its high aspect ratio and surface charge. For further application, the stability of MWNT suspension must be considered. As shown in Figure 23, UV-vis spectrometer of absorbance against time is established for MWNT at the wavelength of 550 nm. It revealed that the absorption of the MWNT-Mica (1mg-2mg in 20 ml solvent) is significantly higher when the mixing process involved with ultrasonication. However, both dispersions are relatively stable over 2 h settlement but with a slightly decreasing in absorption.

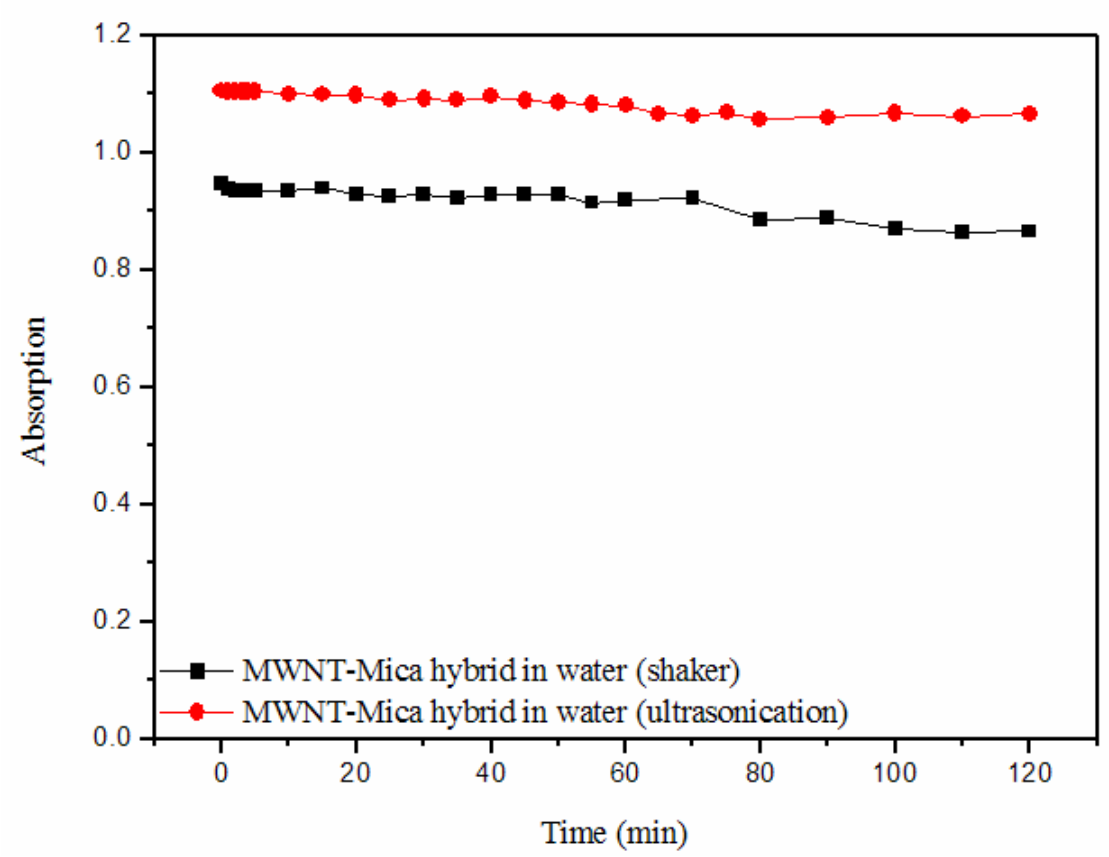

Figure 23. Stability of MWNT-Mica hybrid ($\alpha = 2$) dispersion in water. (3 mg MWNT-Mica hybrid /20 g water)

In polymer process, temperature variable is the major control factor for whole procedure. The influence of temperature on MWNT dispersion was examined. 3 mg MWNT-Mica hybrid (α = 2) dispersed in 20 g water. Based on UV-vis spectrometer, the absorption of the MWNT suspension is very stable and maintained the same value at 20°C~60°C, but with a slightly decreasing at 60°C~80°C (Figure 24).

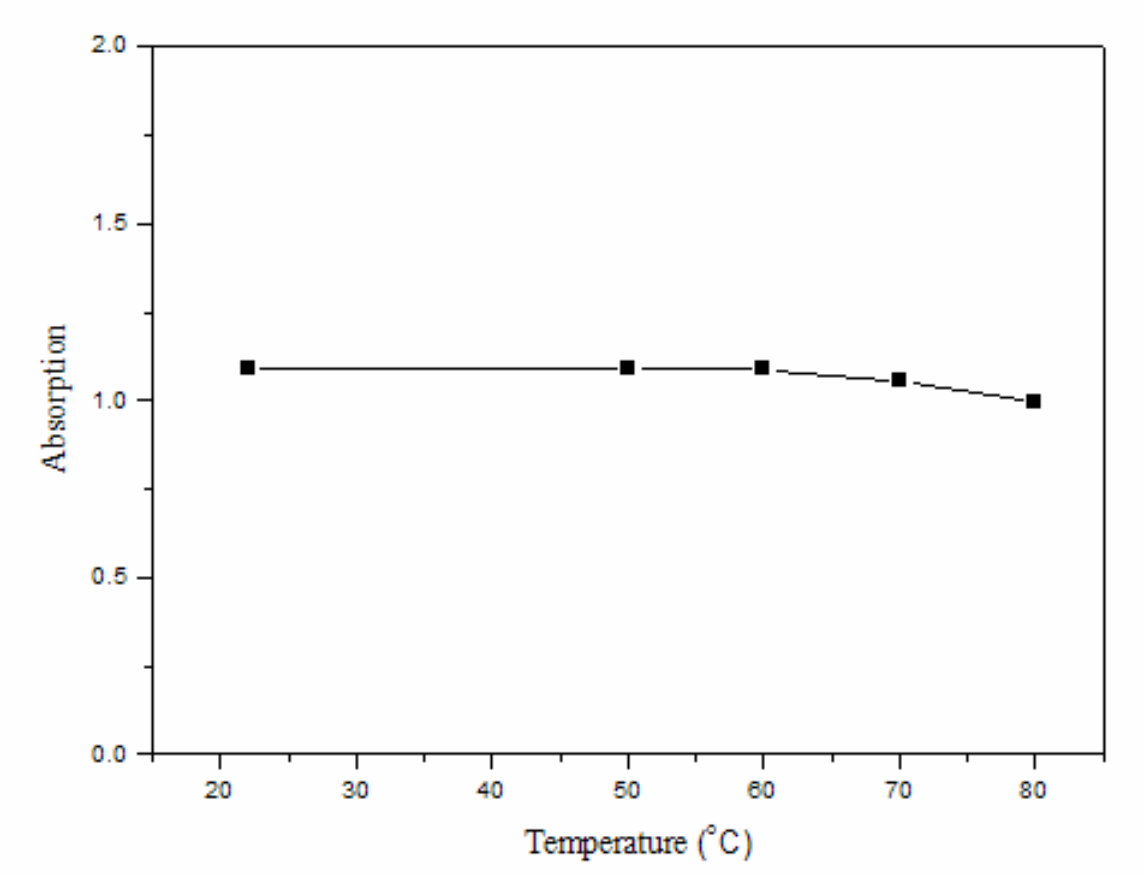

Figure 24. The influence of temperature on MWNT-Mica hybrid (α = 2) dispersion. (3 mg MWNT-Mica hybrid /20 g water)

4.4. Dispersion of MNT-Mica hybrid in Solvents

For comparison, Mica itself can be easily dispersed in common solvents, including H_2O, ethanol, isopropyl alcohol (IPA), acetone, methyl ethyl ketone (MEK), tetrahydrofuran (THF), dimethyl formamide (DMF), dimethyl aceticamide (DMAC) and toluene, at the concentration of 2 mg/20 ml without sedimentation, while the CNT is not dispersible particularly in water. Summarized in Table 4, the results indicate that the MNT-Mica hybrid after thoroughly grounding and ultrasonation become dispersible.

Table 4. Dispersion of MWNT, Mica and MWNT-Mica hybrid in various solvents.

Solvents	Mica[1]	MWNT[2]	MWNT-Mica hybrid[3]
H_2O	○	×	○
Ethanol	○	△*	○*
IPA	○	△*	○*
Acetone	○	△*	○*
MEK	○	△*	○*
THF	○	△*	○*
DMF	○	△*	○
DAMC	○	△*	○
Toluene	○	△*	○*

○ : Dispersed well by shaking only, △* : Dispersed sluggishly, even by both shaking and ultrasonic procedures, × : Poor dispersion or sedimentation, *: Dispersed by shaking and ultrasonication,

[1] 2 mg pristine Mica dispersion in 20 g solvents, [2] 1 mg pristine MWNT dispersion in 20 g solvents, [3] 3 mg MWNT-Mica hybrid ($\alpha = 2$) dispersion in 20 g solvents.

Furthermore, the optimal weight of MNT-Mica hybrid (α = 2) dispersion in solvents also were estimated (Figure 25). The optimal weight for dispersion is 3 mg hybrid in 1 g water, 75 mg hybrid in 1 g DMAC and 80 mg hybrid for 1 g DMF. The result showed that the dispersion of DMF and DMAC are better than water. Compared to the chemical structures of solvents, the excellent dispersion of DMF and DMAC perhaps was due to the amide group. The favorable interaction between MWNT and alkyl amide solvents may account for the polarizability and the optimal geometries.[105]

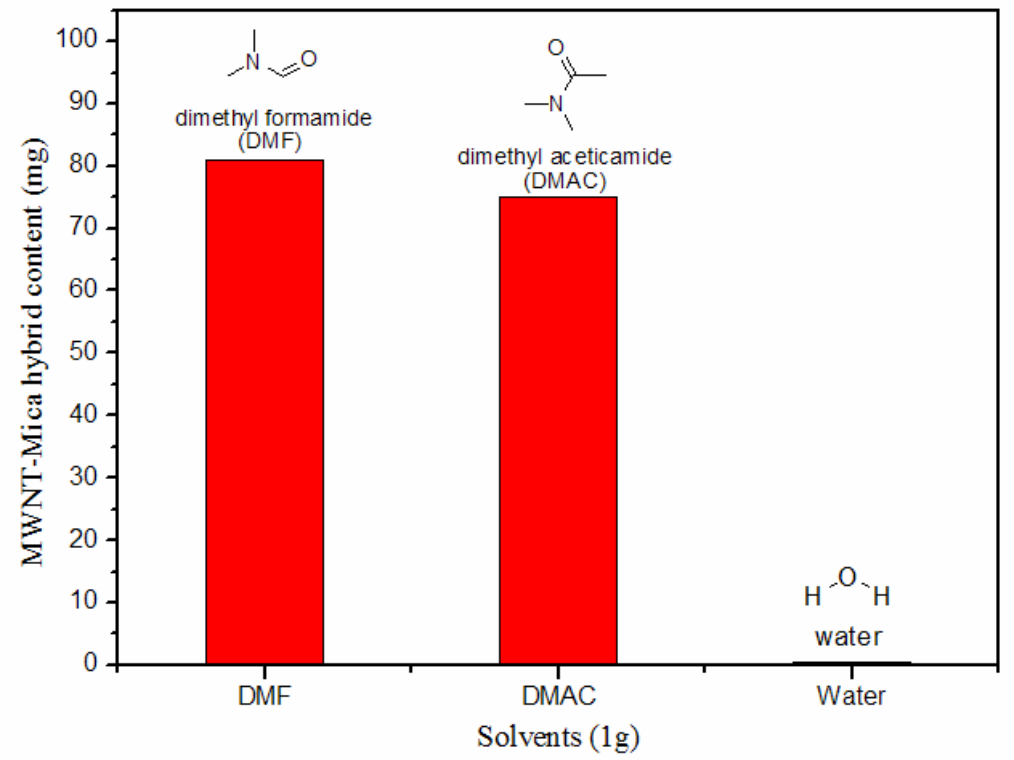

Figure 25. Optimal weight of MWNT-Mica hybrid (α = 2) dispersed in solvents.

4.5. Amphiphillic Nature of MWNT-Mica Dispersion and Irreversible Dispersion Phenomenon

It was found that the MWNT-Mica hybrid (α = 2) are amphiphilic for dispersing in polar and non-polar solvents. Furthermore, the dispersing property is irreversible depended its sequence of exposing to either water or toluene first. In Figure 23, there exhibited two different types of dispersions but derived from the same batch of MWNT-Mica ground powder (α = 2). When the hybrid was dispersed in water first and followed by the toluene addition, the black MWNT-Mica settlement appeared in water phase as shown in Figure 26(A). (Supporting information A: showing the fast toluene/water settling). By mixing to the toluene/water in a reverse order, the same hybrid powder was dispersed first in toluene and then water, each step with agitation by ultrasonication. This time the suspension favored the toluene phase but leaving the bottom water as clear and transparent (Figure 26(B)).

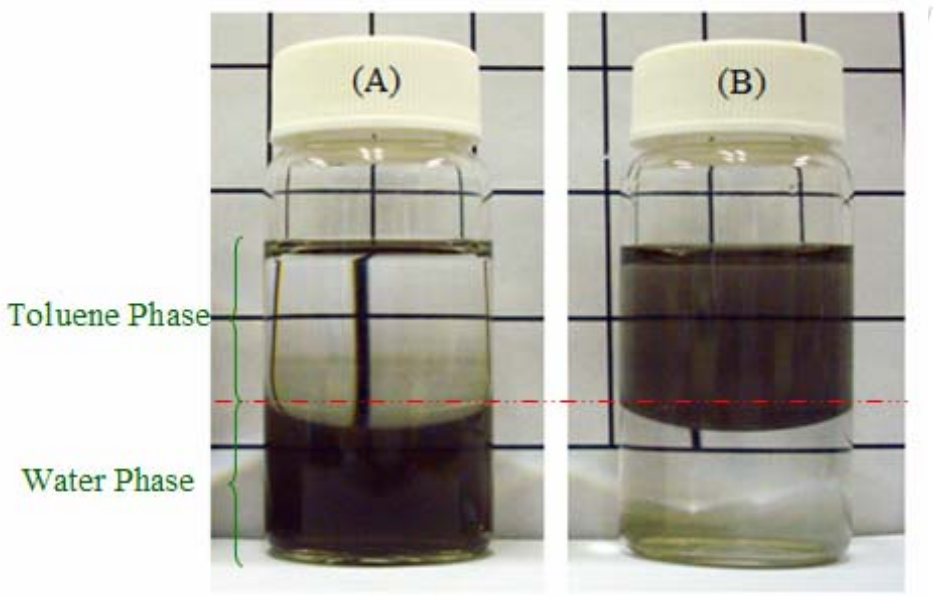

Figure 26. Irreversible dispersion of MWNT-Miac hybrid (α = 2) in (A) water phase, (B) toluene phase.

The water and toluene suspensions were examined by TEM (Figure 27). In the water suspension from the sample of Figure 26(A), individual MWNT and well dispersed Mica can be observed (Figure 27(A)). The enlarged TEM shows the primary structure of MWNT which is coated by Mica (Figure 27(B)). Since MWNT is considered to be hydrophobic and Mica is hydrophilic, the CNT-Mica arrangement is like an oil-in-water micelle structure and thus stable in water as the continuous phase. On the contrary, when the MWNT -Mica was dispersed in toluene, the Mica layer was diffused into the inner aggregation and MWNT appeared in the surrounding phase (Figure 27(C)). The higher magnification of TEM shows the primary structure of MWNT without the Mica coating (Figure 27(D)).

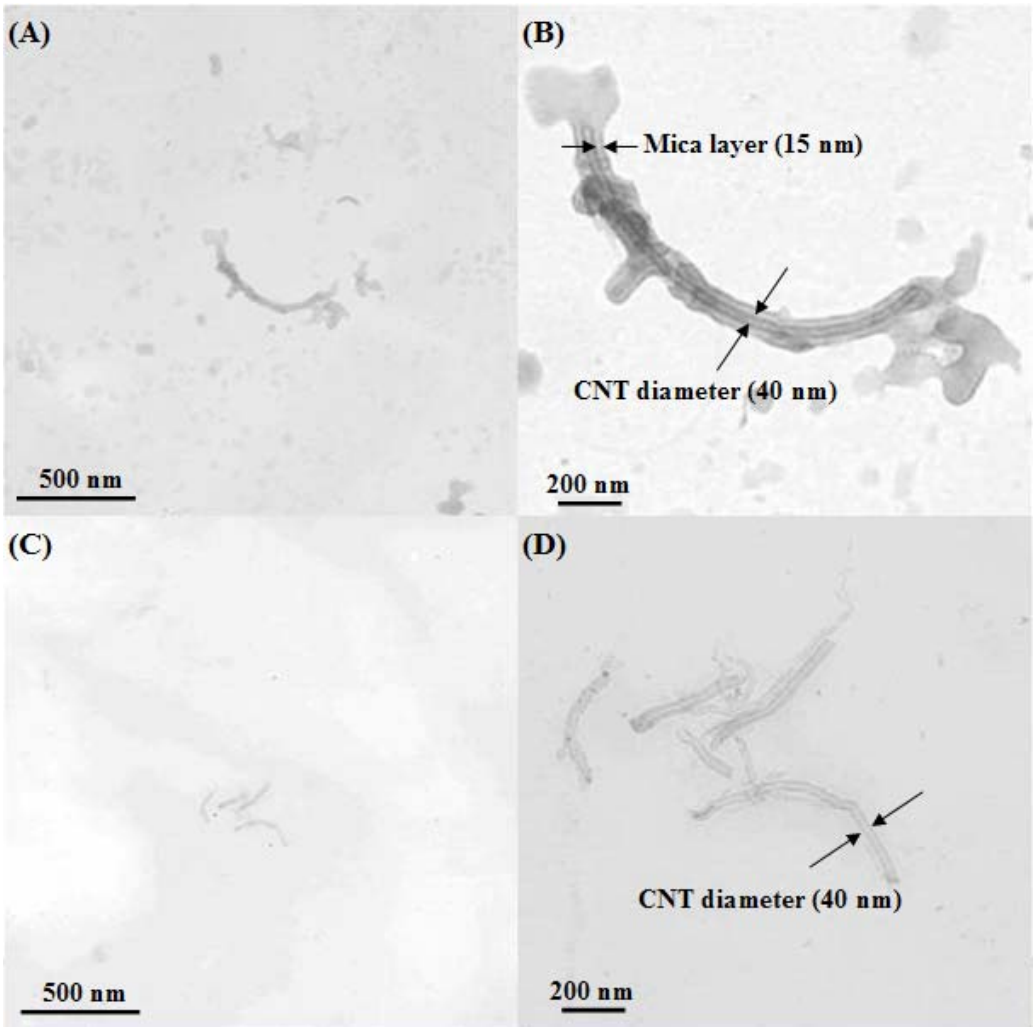

Figure 27. TEM observations of hybrid ($\alpha = 2$) in water (A, B) and toluene (C,D)

4.6. Mechanism of Geometric Shape Influencing Dispersion.

According to the observation of amphiphilic dispersion in water or toluene and TEM observation, we proposed a mechanism to account for these dispersing phenomena, conceptually illustrated in Figure 28. Since Mica is hydrophilic and swelled easily in water, its interaction with CNT may consequently mitigate the original van der Waals attractions and thus the entanglement of the nanotubes. Due to the geometric shape difference, the interference may well derive from the steric hindrance between the fiber-like CNTs and platelet-like Mica clays.

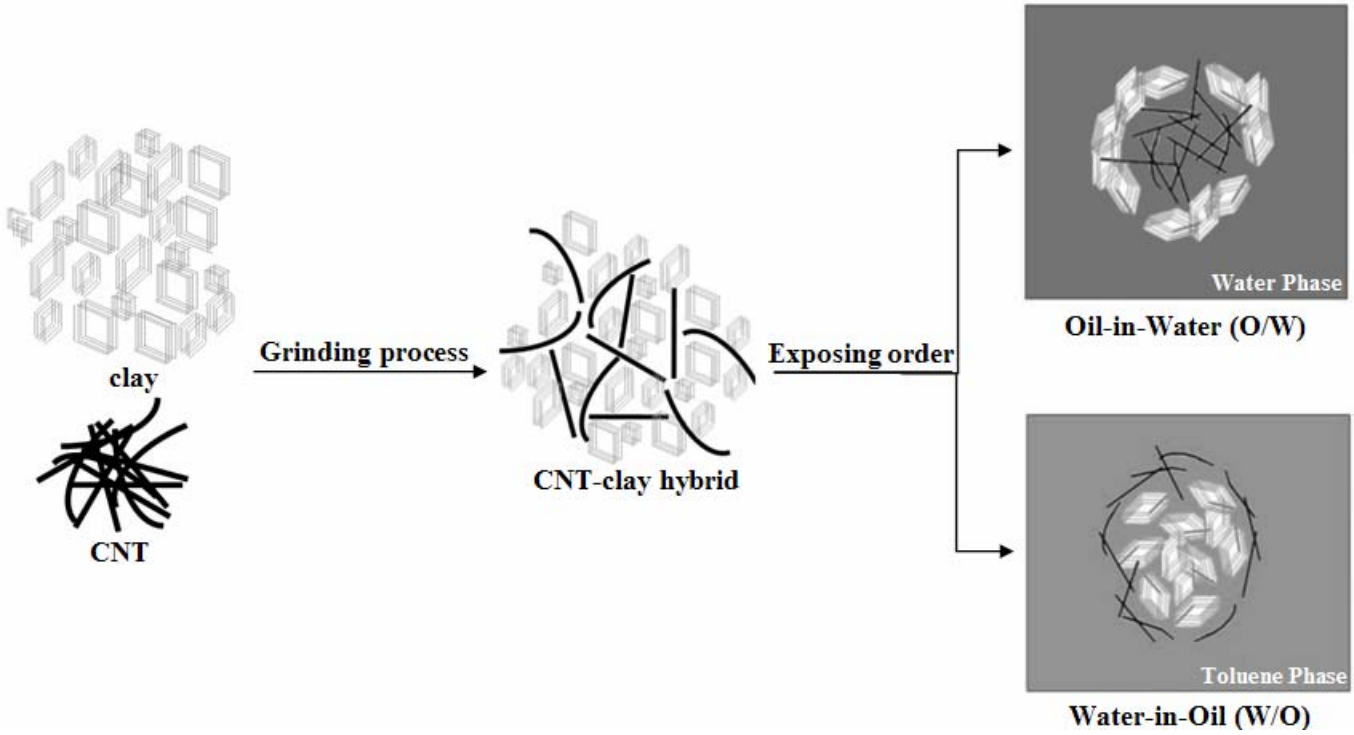

Figure 28. The mechanism of geometric shaped dispersion.

According to the surfactant principle of O/W and W/O micelle formation, a mechanism of geometric shaped dispersion was proposed and further verified by TGA. As shown in Figure 29, Pristine Mica has a good thermal stability below 800°C, while pristine MWNT is unstable above 550°C. The hybrid (MMH2) has the same thermal stability as pristine MWNT and behaves unstable under 550°C. Hybrid from the same bath were dispersed in toluene and water, and sequentially separated from mediates by filter in vacuum. MMH2 which obtained from toluene and water mediate were examined by TGA and the following thermal stability was observed: MMH2 (water) > MMH2 > MMH2 (toluene). The results proved that the conformation of MWNT-Mica hybrid is enable to be manipulated and forms Mica-MWNT and MWNT-Mica (core-shell) micelles.

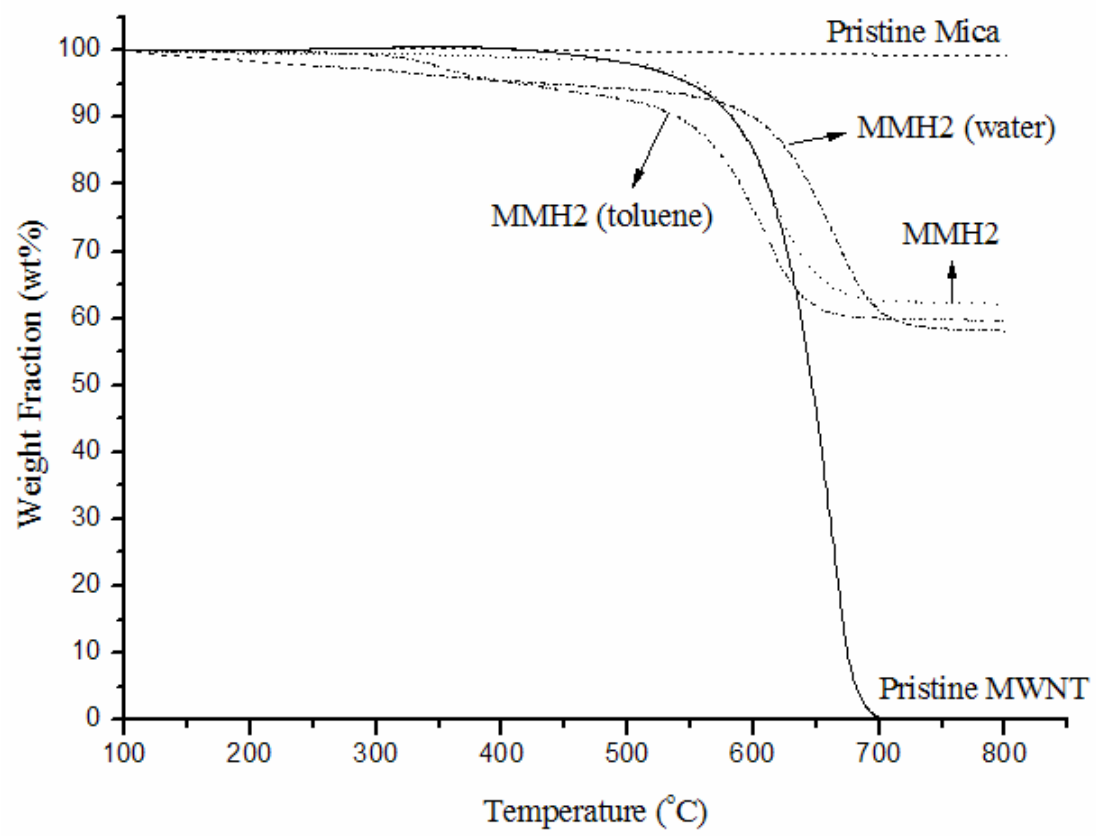

Figure 29. Thermal analysis of MWNT, Mica and MWNT-Mica hybrid (α = 2). (Temperature gradient is 10°C/min in air flow, MMH2 is MWNT-Mica hybrid (α = 2), MMH2 (toluene) is MMH2 suspense in toluene then separated by filter in vacuum, MMH2 (water) is MMH2 suspense in water then separated by filter in vacuum)

4.7. PVA Composites

PVA composites were prepared as described previously. MWNT-Mica hybrid can easily disperse in PVA solution via the conception of geometric shaped dispersion (O/W type dispersion), and the suspensions were black, viscous and homogenous (Figure 30(A)). Mica can easily suspend in PVA solution due to the hydrophilicity of Mica, and formed a white cloudy, viscous and homogeneous suspension. The geometric conception was also applied in the dispersion of pristine MWNT in PVA solution (Figure 31 and Figure 30(C)). Compared to Figure 30(C), MWNT without grinding with PVA were difficult to disperse (Figure 30(D)).

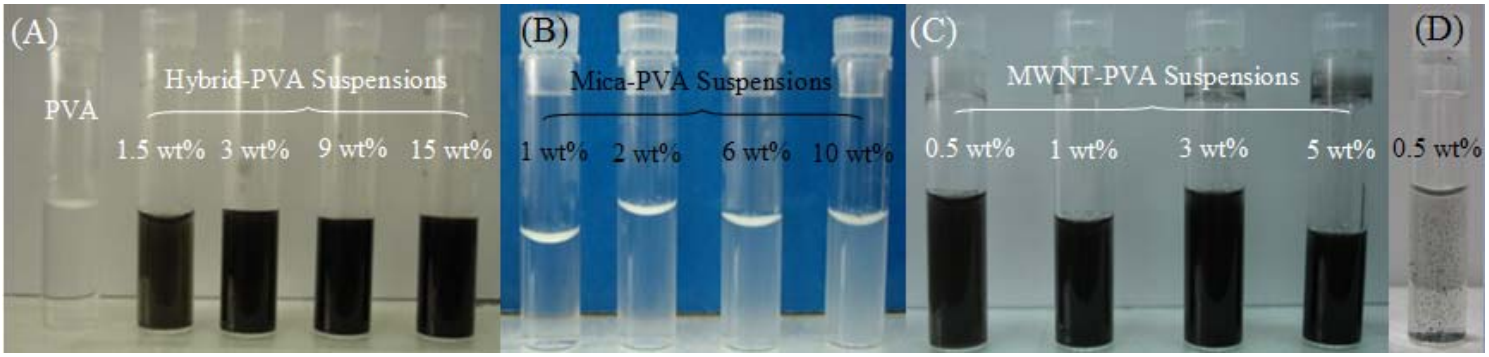

Figure 30. PVA suspensions: (A) Hybrid-PVA suspensions, (B) Mica-PVA suspensions, (C) and (D) are MWNT-PVA suspensions. ((A), (B) and (D) were prepared through Method I and (C) were prepared through Method II)

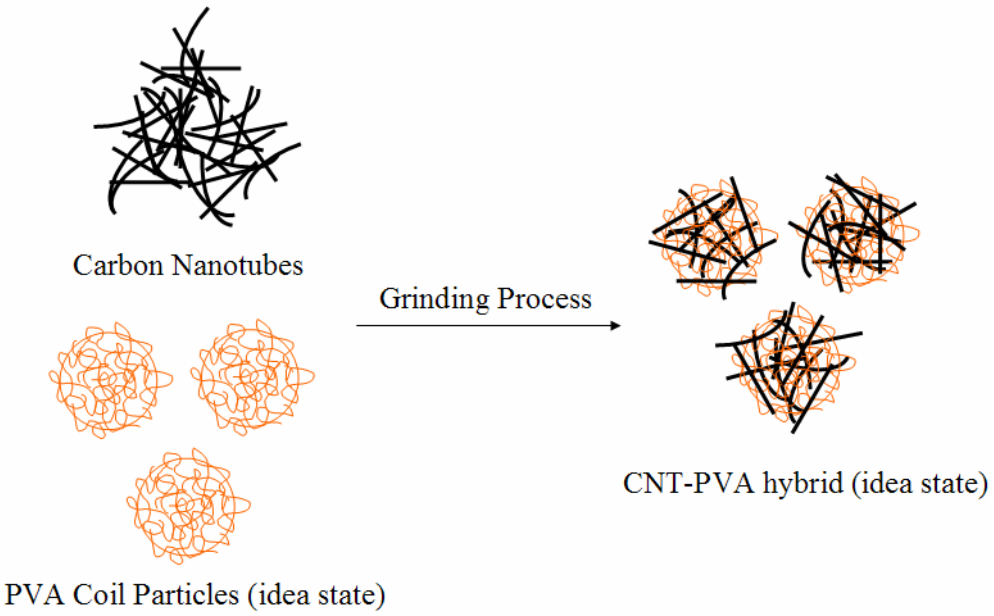

Figure 31. Conceptual presentation of CNT-PVA hybrid.

After hydration, the PVA composites were obtained and thermo-oxidative stability was examined by using a TGA (Figure 32). The hybrid-PVA composites had a slightly lower thermal degradation temperature than the pristine PVA, however, beyond the 50 wt% thermal degradation temperature under air atmosphere, the MWNT-Mica hybrid started to play a role for stabilizing the PVA matrix and the degradation temperature greatly delayed from 300°C (pristine PVA) to 400°C (15 wt% hybrid). The thermo-oxidative stability of Mica-PVA composites and MWNT-PVA hybrid composites were shown in Figure 33 and Figure 34. Both had a slightly lower thermal degradation temperature than the pristine PVA and a slightly delay beyond 50 wt% loss under air flow. Above 450°C, the thermo-oxidative stability of Mica-PVA and MWNT-PVA composites decayed with the increasing amount of Mica and MWNT.

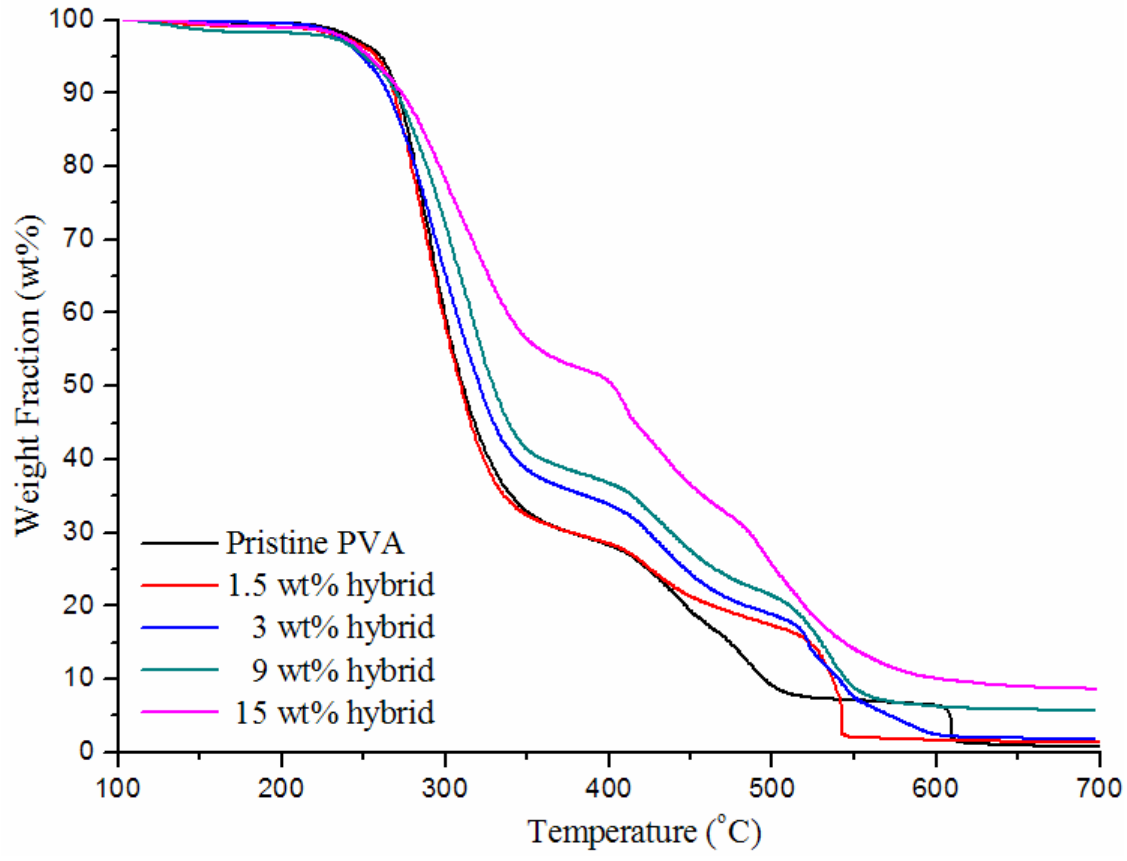

Figure 32. TGA of MWNT-Mica hybrid dispersed in PVA.

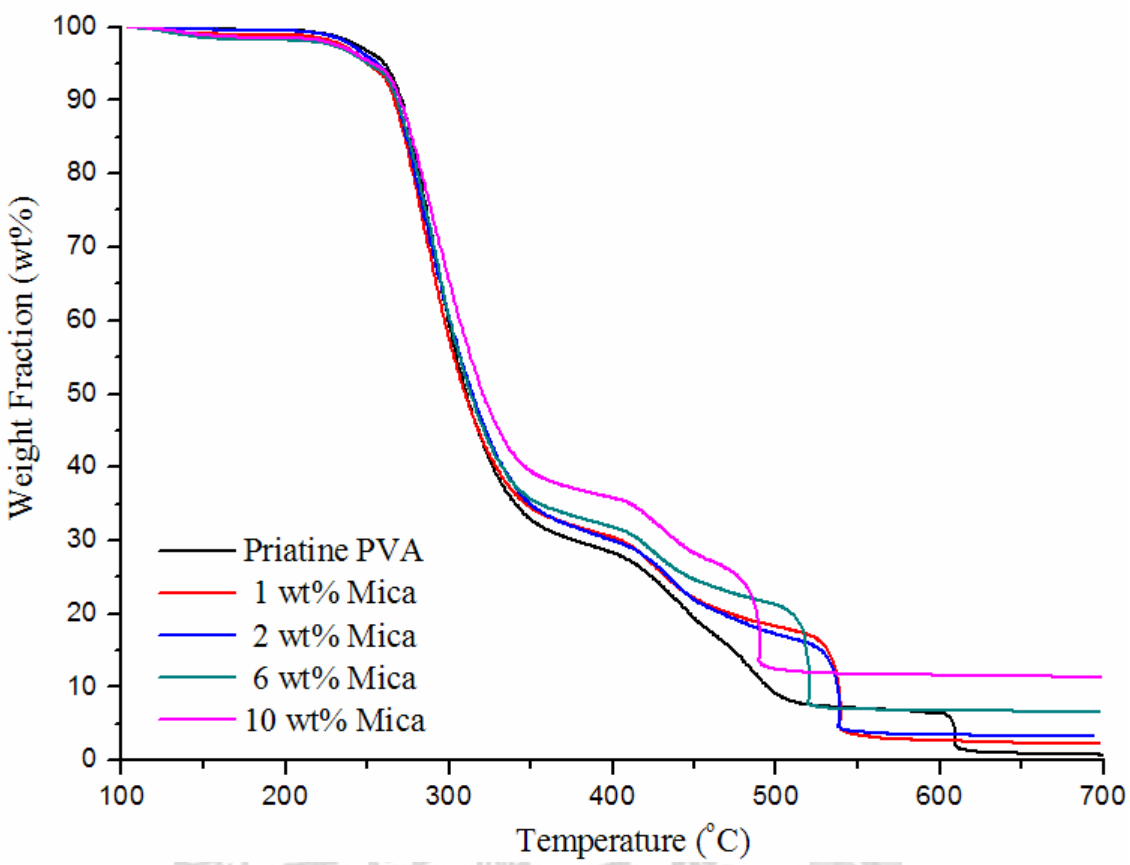

Figure 33. TGA of Mica dispersed in PVA.

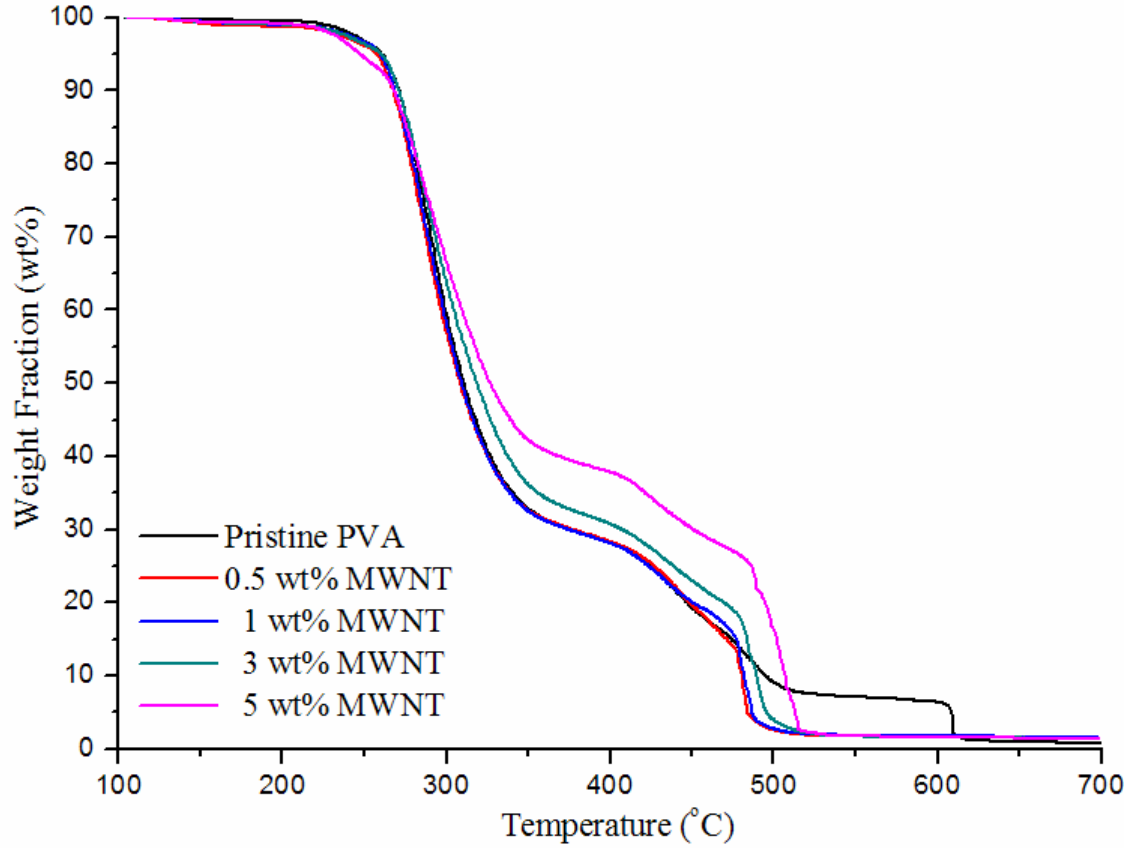

Figure 34. TGA of MWNT dispersed in PVA.

Hybrid-PVA composites were compared with Mica-PVA and MWNT-PVA composites (Figure 35). At low concentration loading, all composites had the same thermo-oxidative stability below 350°C, however, hybrid-PVA and Mica-PVA composites had a delay from 450°C to 550°C (Figure 35(A)). At middle amount loading (Figure 35(B) and (C)), the Hybrid-PVA composites had better thermo-oxidative stability than the others. At higher loading, the Hybrid-PVA composites had excellent thermo-oxidative stability due to the well dispersion and appreciate loading of MWNT-Mica hybrid. Based on the same loading, the Hybrid-PVA composites still have better thermo-oxidative stability than Mica-PVA and MWNT-PVA composites (Figure 36).

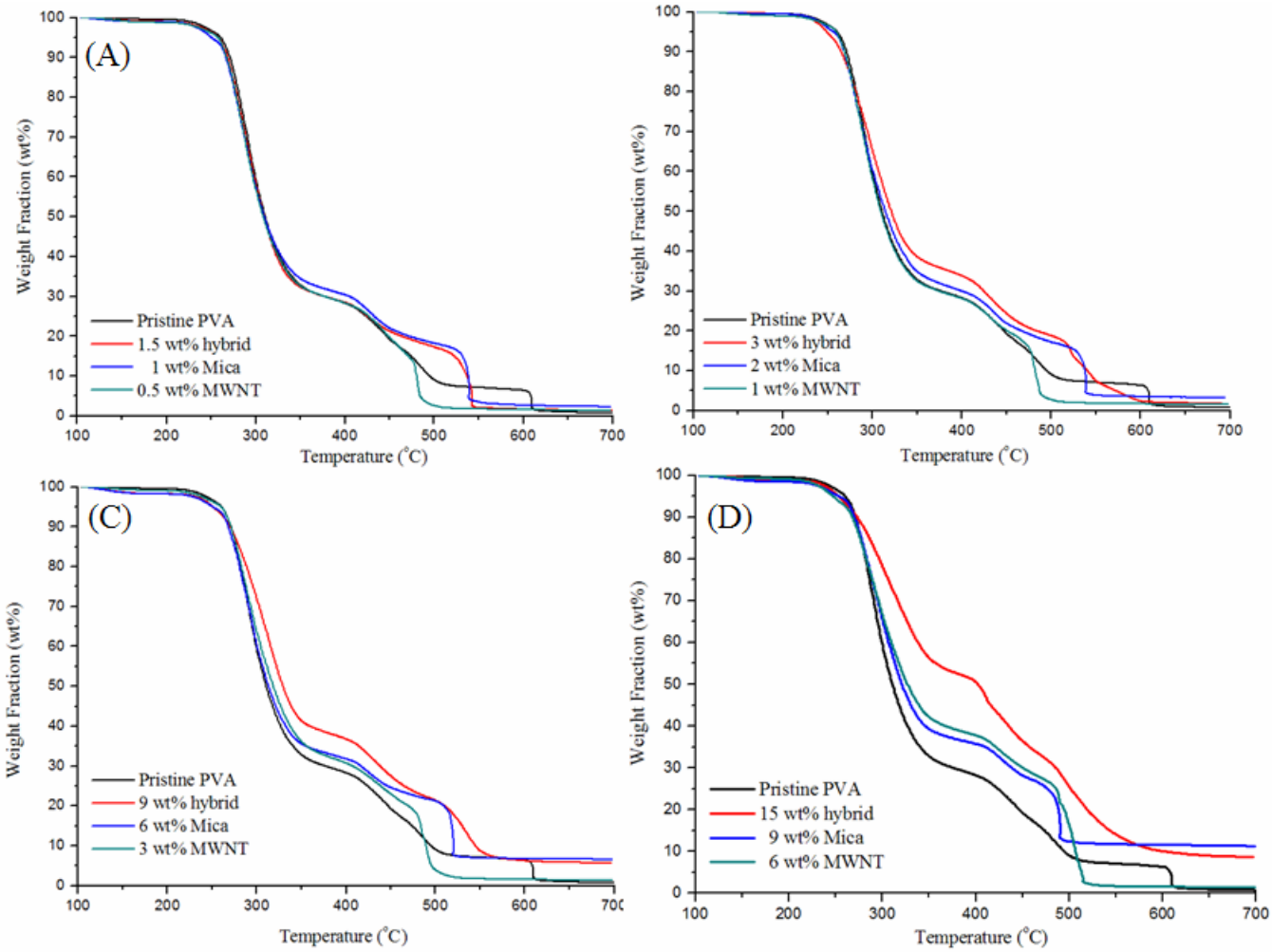

Figure 35. Thermo-oxidative stability of pristine PVA, Hybrid-PVA composites, Mica-PVA composites and MWNT-PVA composites.

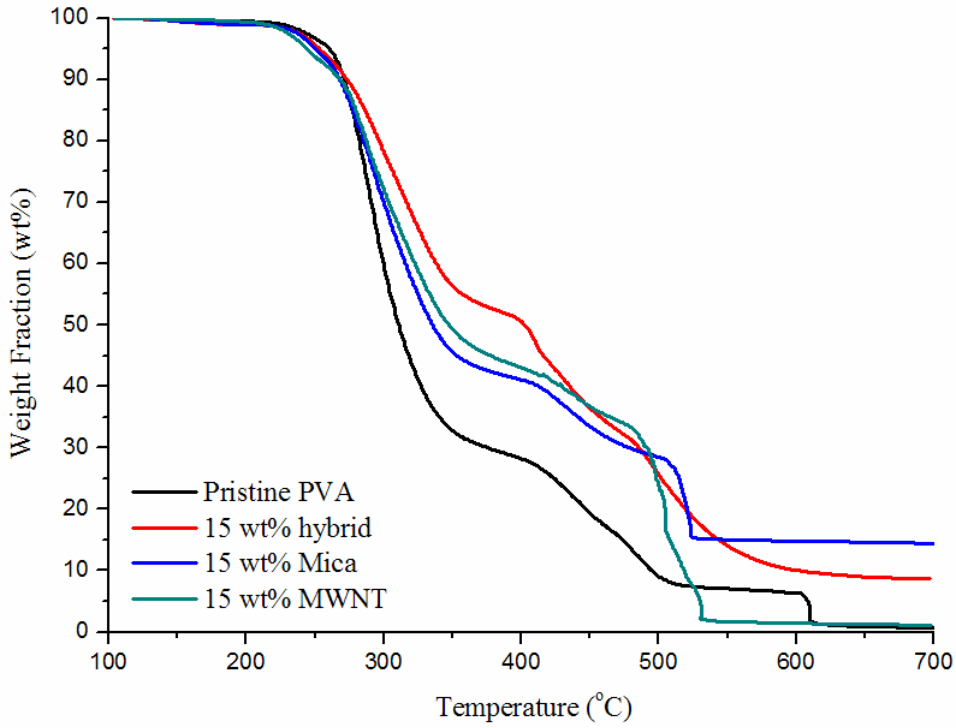

Figure 36. Thermo-oxidative stability of pristine PVA, Hybrid-PVA composites, Mica-PVA composites and MWNT-PVA composites base on the same loading.

5. Conclusion

A convenient dispersion method was developed by grinding MWNT with Mica into fine powder and followed by ultrasonication to disperse the MWNT-Mica hybrid. The combined nanomaterials exhibit a unique amphiphilic property, dispersible in hydrophilic and hydrophobic solvents but depending on the solvent exposing order. The MWNT -Mica hybrid is amphiphilic for both solvent, however, irreversible in process. A proposed mechanism of forming MWNT-Mica and Mica-MWNT core-shell micelles, resembling to the microphase separation of oil-in-water and water-in-oil surfactant micelles, is proposed. The MWNT-Mica hybrid-PVA composites were demonstrated and had a delay of degradation from 300 to 400^{o}C at 50 wt% loss. The MWNT dispersion without using a common organic dispersant could broaden up the nanomaterial applications such as self-assembly, energy development (e.g. fuel cell and hydrogen storage, etc), nanocomposities (e.g. polyvinyl acetate, conducting polymer and epoxy resin, etc.) and bio-medical sensor, etc. Furthermore, the uses of materials with different geometric shapes for dispersion also can be applied in the dispersion of cement, carbon black, TiO_2 particles and pigments, etc.

6. References

[1] J. J. Lin; C. C. Chou; F. S. Shieu, *Macromolecules,* **2003**, 36, 2187.

[2] M. S. Shaffer; R. X. Fan; A. H. Windle, *Carbon,* **1998**, 36, 1603.

[3] S. L. Ren; S. L. Yang; Y. P. Zhao, *Langmuir,* **2004**, 20, 3601.

[4] J. L. Bahr; E. T. Mickelson; M. J. Bronikowski; R. E. Smalley; J. M. Tour, *Chem. Commun.*, **2001**, 193.

[5] K. D. Ausman; R. Piner; O. Lourie; R. S. Ruoff; M. Korobov, *J. Phys. Chem. B*, **2000**, 104, 8911.

[6] F. Takanori, K. Astuko; Y. Ishimura; T. Yamamoto; T. Takigawa; N. Ishii; T. Aida, *Science*, **2003**, 300, 2072.

[7] B. K. Price; J. L. Hudson; J. M. Tour, *J. Am. Chem. Soc.*, 2005, 127, 14867.

[8] H. Kroto, *Science*, **1988**, 242, 1139.

[9] R. F. Curl; R. E. Smalley, *Science*, **1988**, 242, 1017.

[10] S. Iijima, *Science*, **1991**, 354, 56.

[11] T. W. Ebbesen; P. M. Ajayan, *Nature*, **1992**, 358, 220.

[12] Endo, *J. Phys. Chem. Solid*., **1993**, *54*, 1841.

[13] T. Guo; P. Nikolaev; A. Thess; D.T. Colbert; R.E. Smalley, *Chem. Phys. Lett*, **1995**, 243, 49.

[14] M. Yudasaka; R. Yamada; N. Sensui; T. Wilkins; T. Ichihashi; S. Iijima, *J. Phys. Chem. B*, **1999**, 103, 6224.

[15] P. C. Eklund; B. K. Pradhan; U. J. Kim; Q. Xiong; J. E. Fischer; A. D. Friedman; B. C. Holloway; K. Jordan; M. W. Smith, *Nano Lett.*, **2002**, 2, 561.

[16] Maser, Chem, *Phys. Lett.*, **1998**, 292, 587.

[17] A.P. Bolshakov; S.A. Uglov; A.V. Saveliev; V.I. Konov; A.A. Gorbunov; W.

Pompe; A. Graff, *Diamond and Related Materials*, **2002**, 11, 927.

[18] M. S. Dresselhaus, Science of Fullerenes and Carbon Nanotubes. (Academic Press inc., 1996)

[19] S. Niyogi, *Acc. Chem. Res.*, **2002**, 35, 1105.

[20] M. Zheng; B. A. Diner, *J. Am. Chem. Soc.*, **2004**, 126, 15490.

[21] J. W. G. Wilder; L. C. Venema; A. G. Rinzler; R. E. Smalley; C. Dekker, *Nature*, **1998**, 391, 59.

[22] T. W. Odom; J. L. Huang; P. Kim; C. M. Lieber, *Nature*, **1998**, 391, 62.

[23] P. M. Ajayan, *Chem. Rev.*, **1999**, 99, 1787.

[24] Yakobson, *Appl. Phys. Lett.*, **1998**, 72, 918.

[25] M. B. Nardelli; B. I. Yakobson; J. Bernholc, *Phys. Rev. B,* **1998**, 57, R4277.

[26] M. B. Nardelli; B. I. Yakobson; J. Bernholc, *Phys. Rev. Lett.*, **1998**, 81, 4656.

[27] P. Zhang; P. E. Lammert; V. H. Crespi, *Phys. Rev. Lett.*, **1998**, 81, 5346.

[28] D J. Yang; Q. Zhang; G. Chen; S. F. Yoon; J. Ahn; S. G. Wang; Q. Zhou; Q. Wang; J. Q. Li, *Phys. Rev. B,* **2002**, 66, 165440.

[29] R. S. Ruoff; Lorents; C. Donald, *Carbon*, **1995**, 33, 925.

[30] M. A. Osman; D. Srivastava, *Nanotechnology*, **2001**, 12, 21.

[31] J. Hone; M. Whitney; C. Piskoti; A. Zettl, *Phys. Rev. B*, **1999**, 59, R2514.

[32] J. Hone; A. Zettl; M. Whitney, *Syn. Meta*., **1999**, 103, 2498.

[33] S. Berber; Y. K. Kwon; D. Tománek, *Phys. Rev. Lett.*, **2000**, 84, 4613.

[34] Z. Yinghuai; A. T. Peng; K. Carpenter; J. A. Maguire; N. S. Hosmane; M. Takagaki, *J. Am. Chem. Soc., **2005***, 127, 9875.

[35] K. Ajima; M. Yudasaka; T. Murakami; A. Maigne; K. Shiba; S. Iijima, *Molecular Pharmaceltics*, **2005**, 2, 475.

[36] Q. Lu; J. M. Moore; G. Huang; A. S. Mount; A. M. Rao; L. L. Larcom; P. C. Ke, *Nano Lett.*, **2004**, 4, 2473

[37] H. M. So; K. Won; Y. H. Kim; B.K. Kim; B. H. Ryu; P. S. Na; H. Kim; J. O. Lee, *J. Am. Chem. Soc.*,**2005**, 127, 11906.

[38] J. N. Wohlstadter, *Adv. Mater.*, **2003**, 15, 1184.

[39] J. Suhr, *Nano Lett.*, **2006**, 6, 219.

[40] T. Kashiwagi, *Polymer*, **2005**, 46, 471.

[41] S. Barrau, *Macromol. Rapid Commun.,* **2005**, 26, 390.

[42] J. N. Wohlstadter; J. L. Wilbur; G. B. Sigal; H. A. Biebuyck; M. A. Billadeau; L. Dong; A. B. Fischer; S. R. Gudibande; S. H. Jameison; J. H. Kenten; J. Leginus; J. K. Leland; R. J. Massey; S. J. Wohlstadter, *Adv. Mater.*, **2003**, 15, 1618.

[43] W. Wu; S. Zhang; Y. Li; J. Li; L. Liu; Y. Qin; Z. X. Guo; L. Dai; C. Ye; D. Zhu, *Macromolecules,* **2003**, 36, 6286.

[44] Z. Wu; Z. Chen; X. Du; J. M. Logan; J. Sippel; M. Nikolou; K. Kamaras; J. R. Reynolds; D. B. Tanner; A. F. Hebard; A. G. Rinzler, *Science*, **2004**, 305, 1273.

[45] I. Efremenko; M. Sheintuch, *Langmuir*, **2005**, 21, 6282.

[46] W. Li; X. Wang; Z. Chen; M. Waje; Y. S. Yan, *Langmuir*, **2005**, 21, 9386.

[47] K. S. Coleman; S. R. Bailey; S. Fogden; M. L. H. Green, *J. Am. Chem. Soc.,* **2003**, 125, 8722.

[48] A. Adronov; Z. Yao; N. Braidy; G. A. Botton, *J. Am. Chem. Soc.,* **2003**, 125, 16015.

[49] I. C. Liu; H. M. Huang; C. Y. Chang; H. C. Tsai; C. H. Hsu; R. C. C. Tsiang, *Macromolecules*, **2004**, 37, 283.

[50] L. Qu; L. M. Veca; Y. Lin; A. Kitaygorodskiy; B. Chen; A. M. McCall; J. W. Connell; Y. P. Sun, *Macromolecules*, **2005**, 38, 10328.

[51] J. Liu; A. G. Rinzler; H. Dai; J. H. Hafner; R. K. Bradley; P. J. Boul; A. Lu; T. Iverson; K. Shelimov; C. B. Huffman; F. R. Macias; Y. S. Shon; T. R. Lee; D. T. Colbert; R. E. Smalley, *Scienec*, **1998**, 280, 1253.

[52] K. A. Williams; P. T. M. Veenhuizen; B. G. de la Torre; R. Eritja; C. Dekker, *Nature,*

2002, 420, 761.

[53] K. Jiang; L. S. Schadler; R. W. Siegel; X. Zhang; H. Zhang; M. Terrones, *J. Mater. Chem.,* **2004**, 14, 37.

[54] M. Guo; J. Chen; D. Liu; L. Nie; S. Yao, *Bioelectrochemistry,* **2004**, 62, 29.

[55] J. Chen; M. A. Hamon; H. Hu; Y. Chen; A. M. Rao; P. C. Eklund; R. C. Haddon, *Scienec*, **1998**, 282, 95.

[56] Y. Qin; L. Liu; J. Shi; W. Wu; J. Zhang; Z. X. Guo; Y. Li; D. Zhu, *Chem. Mater.*, **2003**, 15, 3256.

[57] H. Kong; C. Gao; D. Yan, *Macromolecules*, **2004**, 37, 4022.

[58] U. D. Weglikowska; V. Skakalova; R. Graupner; S. H. Jhang; B. H. Kim; H. J. Lee; L. Ley; Y. W. Park; S. Berber; D. Tomanek; S. Roth, *J. Am. Chem. Soc.,* **2005**, 127, 5125.

[59] L. Xudong; D. Christophe; S. Valérie; P. Christophe, *Polymer*, **2004**, 45, 6097.

[60] A. Adronov; Y. Liu; Z. Yao, *Macromolecules*, **2005**, 38, 1172.

[61] S. Qin; D. Qin; W. T. Ford; J. E. Herrera; D. E. Resasco, *Macromolecules*, **2004**, 37, 9963.

[62] S. Qin; D. Qin; W. T. Ford; D. E. Resasco; J. E. Herrera, *J. Am. Chem. Soc.*, **2004**, 126, 170.

[63] S. Qin; D. Qin; W. T. Ford; D. E. Resasco; J. E. Herrera, *Macromolecules*, **2004**, 37, 752.

[64] H. Kong; C. Gao; D. Yan, *J. Am. Chem. Soc.*, **2004**, 126, 412.

[65] G. Gao, *Macromolecules*, **2005**, 38, 8634.

[66] Hao. Kong; P. Luo; C. Gao; D. Yan, *Polymer*, **2005**, 46, 2472.

[67] D. Chattopadhyay; I. Galeska; F. Papadimitrakopoulos, *J. Am. Chem. Soc.,* **2003**, 125, 3370.

[68] Y. Maeda; S. Kimura; Y. Hirashima; M. Y. Kanda; Y. Lian; T. Wakahara; T. Akasaka; T. Hasegawa; H. Tokumoto; T. Shimizu; H. Kataura; Y. Miyauchi; S.

Maruyama; K. Kobayashi; S. Nagase, *J. Phys. Chem. B*, **2004**, 108, 18395.

[69] N. Choi; M. Kimura; H. Kata, *Jpn. J. Appl. Phys.*, 2002, 41, 6264.

[70] H. Chang; J. D. Lee; S. M. Lee; Y. H. Lee, *Appl. Phys. Lett.*, **2001**, 79, 3863.

[71] J. Kong; H. Dai, *J. Phys. Chem. B,* **2001**, 105, 2890.

[72] K. Bradley; J. C. P. Gabriel; M. Briman; A. Star; G. Grüner, *Phys. Rev. Lett.*, **2003**, 91, 218301.

[73] E. V. Basiuk; V. A. Basiuk; J. G. Banuelos; B. J. M. Saniger; V. A. Pokrovskiy; T. Y. Gromovoy;A. V. Mischanchuk; B. G. Mischanchuk, *J. Phys. Chem. B*, **2002**, 106, 1588.

[74] V. C. Moore; M. S. Strano; E. H. Haroz; R. H. Hauge; R.E. Smalley; J. Schmidt; Y. Talmon, *Nano Lett.*, **2003**, 3, 1379.

[75] H. T. Ham; Y. S. Choi; I. J. Chung, *J. Colloid Interface Sci.*, **2005**, 286, 216.

[76] X. Lou; R. Daussin; S. Cuenot; A. S. Duwez; C. Pagnoulle; C. Detrembleur; C. Bailly; R. Jerome, *Chem. Mater.,* **2004**, 16, 4005.

[77] O. K.Kim; J. Je; J. W. Baldwin; S. Kooi; P. E. Pehrsson; L. J. Buckley, *J. Am. Chem. Soc.,* **2003**, 125, 4426.

[78] V. A. Sinani; M. K. Gheith; A. A. Yaroslavov; A. A. Rakhnyanskaya; K. Sun; A. A. Mamedov; J. P. Wicksted; N. A. Kotov, *J. Am. Chem. Soc.,* **2005**, 127, 3463.

[79] A. Carrillo; J. A. Swartz; J. M. Gamba; R. S. Kane; N. Chakrapani; B. Wei; P. M. Ajayan, *Nano Lett.*, **2005**, 3, 1437.

[80] A. Star; D. W. Steuerman; J. R. Heath; J. F. Stoddart, *Angew. Chem.*, **2002**, 41, 2508.

[81] S. Iijima, *Appl. Phys. A,* **2000**, 71, 449.

[82] T. A. Taton; Y. Kang, *J. Am. Chem. Soc.,* **2003**, 125, 5650.

[83] H. Kitano; K. Tachimoto; T. N. Hirabayashi; H. Shinohara, *Macromol. Chem. Phys.*, **2004**, 205, 2064.

[84] J. F. Stoddart, *Angew. Chem.*, **2001**, 113, 1771.

[85] J. F. Stoddart ; A. Star; J. F. Stoddart; D. Steuerman; M. Diehl; A. Boukai; E. W. Wong; X. Yang; S. W. Chung; H. Choi; J. R. Heath, *Angew. Chem.*, **2001**, 40, 1721.

[86] R. E. Smalley, *Chem. Phys. Lett.*, **2001**, 342, 265.

[87] J. F. Stoddart; A. Star; Y. Liu; K. Grant; L. Ridvan; J. F. Stoddart; D. W. Steuerman; M. R. Diehl; A. Boukai; J. R. Heath, *Macromolecules*, **2003**, 36, 553.

[88] F. Balavoine; P. Schultz; C. Richard; V. Mallouh; T. W. Ebbesen; C. Mioskowski, *Angew. Chem. Int. Ed.*, **1999**, 38, 1912.

[89] C. Y. Li; L. Li; W. Cai; S. L. Kodjie; K. K. Tenneti, *Adv. Mater.*, **2005**, 17, 1198.

[90] M. Shim; W. S. Kam; R. J. Chen; Y. Li; H. Dai, *Nano Lett.*, **2002**, 2, 285.

[91] K. Bradley; M. Briman; A. Star; G. Gruner, *Nano Lett.*, **2004**, 4, 253.

[92] Z. Guo; P. J. Sadler; S. C. Tsang, *Adv. Mater.*, **1998**, 10, 701.

[93] P. J. Sadler, *J. Am. Chem. Soc. Comrnun.*, 1995, 1803.

[94] P. J. Sadler, *Angew. Chem. Int. Ed. Engl.*, **1997**,36, 2198.

[95] P. J. Sadler, *Angew. Chem.*, **1997**,109, 2291.

[96] G. R. Dieckmann; A. B. Dalton; P. A. Johnson; J. Razal; J. Chen; G. M. Giordano; E. Munoz; I. H. Musselman; R. H. Baughman; R. K. Draper, *J. Am. Chem. Soc.*, **2003**, 125, 1770.

[97] V. Zorbas; A. O. Acevedo; A. B. Dalton; M. M. Yoshida; G. R. Dieckmann; R. K. Draper; R. H. Baughman; M. J. Yacaman; I. H. Musselman, *J. Am. Chem. Soc.*, **2004**, 126, 7222.

[98] A. O. Acevedo; H. Xie; V. Zorbas; W. M. Sampson; A. B. Dalton; R. H. Baughman; R. K. Draper; I. H. Musselman; G. D. Dieckmann, *J. Am. Chem. Soc.*, **2005**, 127, 9512.

[99] [a] M. Alexandre, P. Dubois, *Mater. Sci. Eng.* **2000**, *28*, 1.

[b] J. J. Lin, Y. M. Chen, *Langmuir* **2004**, *20*, 4261.

[100] J. F. Dobkin; J. R. Saha; V. P. Butler; H. C. Neu; J. Lindenbaum, *Science* **1983**, *220*, 365.

[101] J. M. H. Emiel, B. Smit *J. Phys. Chem. B* **2002,** *106,* 12664.

[102] M. Meyn; K. Beneke; G. Lagaly, *Inorg. Chem.* **1990,** *29*, 5201.

[103] D. Baskaran; J. W. Mays; M. S. Bratcher, *Chem. Mater.*, **2005**, 17, 3389.

[104] T. Yongqiang, R. Daniel, *J. Phys. Chem. B*, **2005**, 109, 14454.

[105] B. J. Landi; H. J. Ruf; J. J. Worman; R. P. Raffaelle, *J. Phys. Chem. B*, **2004**, 108, 17089.